4. HYDROXYAPATITE FIBERS FROM ELECTROSPUN PVA/INORGANIC SOL MIXTURES

The results obtained on the development of the procedure were submitted for publication in the *Journal of Materials Science*. This paper is currently under review and is attached in the following pages.

Hydroxyapatite fibers from electrospun PVA/inorganic sol mixtures

Xiaoshu Dai, Satya Shivkumar*

Department of Mechanical Engineering,
Worcester Polytechnic Institute,
100 Institute Road,
Worcester, MA01609

+1-508-831-5681

*Email: shivkuma@wpi.edu

4.1 ABSTRACT

PVA with an average molecular weight between 50,000 and 124,000 g/mol was electrospun with a Calcium Phosphate based sol. The sol was prepared by reacting Triethyl Phosphite and Calcium Nitrate and was directly added to an aqueous solution of PVA. This mixture was electrospun at a voltage of 20 - 30 kV. The results indicate that the sol was distributed uniformly in the PVA fibers, whose diameter was on the order of 2 μm. This electrospun structure was calcined at 600^{o}C for 6 hr to obtain a residual inorganic, sub-micron fibrous network. X-ray diffraction of this fibrous structure indicated that it consisted predominantly of hydroxyapatite with an average crystal size of almost 30 nm. Dense or micro-porous hydroxyapatite fibers and scaffolds could be obtained by varying the polymer molecular weight and the polymer/sol ratio. The micro-porous fibers can have many potential uses in the repair and treatment of bone defects, drug delivery and tissue engineering.

Key Words:
Hydroxyapatite, fibers, electrospinning

4.2 INTRODUCTION

Synthetic hydroxyapatite (HA) particles, films, coatings, fibers and porous skeletons are used extensively in various biomedical applications [1]. This bioceramic, $Ca_{10}(PO_4)_6(OH)_2$, can be synthesized by many wet chemical and mechano-chemical methods [2,3]. The sol-gel route is becoming a common technique to produce ultra fine and pure ceramic powders [4,5]. Various methods have been developed to introduce porosity in HA scaffolds including incorporation of volatile organic particles [6], gel casting [7], replication of a polymer sponge [8] and salt leaching [9,10]. The sol-gel technique is also being used in conjunction with various spinning techniques to produce ceramic fibers. Ramanan *et al.* [11] have used a calcium phosphate sol in a rotating spinnerette system to produce HA fibers. Several researchers have used electrospinning for the production of macro-porous ceramic structures containing a network of submicron fibers [12-15]. A variety of ceramic fibers, with average diameters in the sub-micron range, including lithium manganese oxide [12], Mn_2O_3 and Mn_3O_4 [13], Barium titanate [14] and silica [15] have been produced by this technique. Typically, the sol is electrospun with a polymer solution and the resultant structure is fired at temperatures on the order of 600 ^oC to remove the polymer. Wu *et al.* [16] have electrospun a calcium phosphate sol with a high molecular weight polymer to produce hydroxyapatite fibers on the order of 10 – 30 μm in diameter. The purpose of this contribution is to examine the effects of the polymer molecular weight and of the polymer-sol ratio on the characteristics of the inorganic fibers produced by the aforementioned technique.

4.3 EXPERIMENT PROCEDURE

Triethyl phosphite (TEP, Aldrich, USA) and calcium nitrate tetrahydrate ($Ca(NO_3)_2{\cdot}4H_2O$, Aldrich, USA) were used as the raw materials for preparing the sol [4,5]. Poly vinyl alcohol (PVA) with various weight average molecular weights (M_W) was obtained from Aldrich Chemical Company, Milwaukee, WI (Table 1). The

ceramic precursor was prepared by a sol-gel routine described previously [5]. Appropriate amounts (11.9 g) of calcium nitrate tetrahydrate (to obtain a Ca/P ratio of 1.67) were dissolved in 10 mL of distilled water. About 5.2 mL of Triethyl phosphite was hydrolyzed with 10 mL of distilled water. The nitrate solution was added dropwise into the hydrolyzed phosphate solution. The resulting mixture was stirred vigorously for 2 hr in an aqueous environment and aged at 80 ^{o}C for 24 hr. A transparent sol was obtained after the aging treatment.

Appropriate amounts of PVA (Table 1) were dissolved in distilled water. The dissolution was conducted in a water bath at 80 ^{o}C, with constant stirring for at least 2 hr to ensure complete dissolution. The electrospinning precursor was prepared by mixing the sol and the polymer solutions at room temperature. The volumetric ratio between the PVA solution and the inorganic sol was varied between 1:5 and 5:1. The mixture was then sealed and vigorous stirring was continued for at least 8 hr at 25 ^{o}C. After this, the stirring was stopped to facilitate the removal of gas bubbles. The viscosity of PVA/sol solutions at 25°C was measured using a digital viscometer (Brookfield Model DV III). The shear rate was varied between 0.1 and 15 s^{-1}.

About 1 mL of this solution was placed in a syringe equipped with an 18 gauge needle (Outer diameter = 1.27 mm, 52 mm long). The syringe was mounted horizontally in a syringe pump (EW-74900-00, Cole-Parmer). The syringe pump was adjusted to achieve a flow rate of about 0.3 mL/hr. A potential of 20 to 30 kV was applied to the needle immediately after a pendant drop formed at the tip of the needle. The grounded collector was positioned at a distance of 10 cm from the tip of the needle and consisted of an aluminum foil 10 cm×10 cm in cross section. The samples obtained after electrospinning were dried at room temperature for at least 8 hr. They were then calcined at 600 ^{o}C for 6 hr.

The samples were sputter coated with gold–palladium and examined in a JSM-840 scanning electron microscope (SEM) with an energy dispersive X-ray detector (EDX)

attachment (Kevex). X-ray diffraction studies were conducted with Cu *K-α* radiation on small samples scraped from the aluminum foil.

4.4 RESULTS AND DISCUSSION

A hygroscopic white solid gel was obtained from the sol after driving off the solvent at 80 ^{o}C for 8 hr (same as the aging temperature). When this gel was calcined at 600 ^{o}C, the weight loss was about 40 wt%, which compares well with the data of Liu *et al.* [4], who have measured the total weight loss after heating from the gel to the calcium phosphate powder to be about 44 wt%. They indicate that this weight loss originates from a) removal of residuals in the temperature range 100 to 300 ^{o}C (18 wt %) and b) nitrate decomposition between 300 to 520 ^{o}C (26 wt %). Increasing the temperature beyond 520 ^{o}C does not seem to produce any additional weight loss. Hence, fthe gel at 600 ^{o}C is likely to produce a non-volatile residue containing predominantly calcium phosphate. It should be noted that when the sol was held at a temperature of 600 ^{o}C for 6 hr, the total weight loss was around 70 wt%. The additional weight loss in the sol (compared to that of the gel) stems from the loss of the solvent. The total weight loss from a PVA/sol mixture (5:1 volume ratio) was measured to be on the order of 81 wt%, indicating that after firing for 6 hr at 600 ^{o}C all the polymer degradation products had volatilized.

The zero shear viscosity of the as-prepared sol was measured to be about 0.006 Pa·s. By comparison, the zero shear viscosity of the PVA solution with 10.7 wt% (M_W = 124,000 - 186.000 g/mol) was on the order of 3.3 Pa·s. Initial attempts to electrospin the pure sol resulted in a range of droplets. Subsequently, the sol was converted to a gel by heating to 80 ^{o}C and driving off the solvent. This white gel was too viscous to disperse into the polymer solution and hence, the polymer-gel combination could not be electrospun successfully. Consequently, in all subsequent experiments, the polymer solution was mixed directly with the sol before electrospinning. The zero

shear rate viscosity of the polymer solution and sol mixture varied from 2.5 Pa·s (PVA/sol ratio of 5:1) and 0.45 Pa.s (PVA/sol ratio of 1:5)

The M_W and the concentration of the polymer in solution had a significant effect on the structure obtained after electrospinning and after firing. The effects of M_W and concentration can be described in terms of the Berry number, ($Be = [\eta]c$) where $[\eta]$ is the intrinsic viscosity and c is the concentration: The intrinsic viscosity can be obtained from the Mark-Houwink equation [17].

$$[\eta] = K(M_w)^a \qquad (1)$$

The Mark-Houwink constants K and a for PVA with water as the solvent have been reported to be 6.51×10^{-6} mL/g and 0.628 respectively [18]. It has been shown that stable fibrous structures can be obtained with pure PVA for $[\eta]c > 5$ [19]. All the experiments in this investigation were conducted at $[\eta]c = 13$. At M_W = 50,000 - 85,000 g/mol, a limited number of fibers were obtained for a polymer/sol volume ratio of 3:1. The fibers started to solidify roughly at a distance that was halfway between the needle tip and the collector. Typically, many thin fibers, with embedded sol particles, joined together to form thick fibers, as can be seen from the layering effect shown in Fig. 1. The structure also contained several fractured fiber fragments and large splats resulting from sprayed droplets. After firing, the thick fibers of polymer/sol mixture could be converted to calcium phosphate fibers whose thickness was on the order of 20 μm as shown in Fig. 1(b). This fiber diameter is comparable to the data of Wu *et al.* [16] who produced 10 mm long Hydroxyapatite fibers with an average diameter between 10 and 30 μm using a similar procedure. When a polymer with a M_W of 124,000 - 186,000 g/mol was used along with a polymer/sol ratio of 3:1, the fibrous structure became more pronounced as shown in Fig. 2. In this case, the polymer solution and the sol may form a partially miscible mixture during sample preparation. When this mixture is electrospun, fibers containing sol particles embedded in a polymer phase with some dispersed sol may be obtained (Fig. 2(a)). The size of the electrospun fibers was on the order of 2 to 5 μm. Upon firing, the sol

particles are converted to a phase that is predominantly hydroxyapatite, shown as bright particles in Fig. 2(b). These particles show up as the bright spots on the X-ray maps shown in Figs 2 (c) and (d). The small fraction of sol that may be dispersed in the polymer solution is also converted to hydroxyapatite, which is indicated by the background brightness in Figs. 2(c) and (d). The average size of the sol particles before and after firing was typically on the order of 3 μm and 2 μm respectively. The white powder remaining after calcination was scratched off from the aluminum foil and analyzed by X-ray diffraction. The diffraction pattern, plotted in Fig. 3(b), shows the characteristic peaks of hydroxyapatite. Some minor phases, most notably, β-tricalcium phosphate and CaO, were also observed in small fractions. The crystal size was calculated from the Scherrer equation [20] to be between 30 and 40 nm.

The data of Zong *et al.* [21] indicate that the addition of an electrolytic salt to polymer solutions may affect the structures attainable after electrospinning. Electrolytes may prevent bead formation and lead to the development of thin fibers. The addition of salts increases the charge density on the surface of the ejected jet and enhances the elongation forces imposed on the jet. Consequently, as the charge density increases, fibers with smaller diameters are obtained. Some of the fibers may also undergo fracture because of elongational flow. Furthermore, the fiber morphology obtained depends on the size of the ions in the electrolyte. Zong *et al.*'s [21] data show that smaller ions generally lead to a larger elongation force, thereby producing spindle-like beads and lower fiber diameter. The results shown in Fig. 4 indicate that the fraction of beads and the fiber diameter decreased upon the addition of the sol to the polymer solution. The inorganic sol in this investigation was likely to contain Ca^{2+}, PO_4^{3-} and NO_3^- ions, which may increase the charge density of the jet, leading to a reduction in the fiber diameter. In low M_W samples, this increased elongational flow upon the addition of the sol may cause the fibers to thin out and fracture (Figs. 4 (a) and (b)). The sol particles may either disrupt the fibrous structure during electrospinning or form big beads within the fibers. By comparison, at high M_W (although at the same

Be), the fiber diameter decreases upon the addition of the sol, but the fibers seem to resist this tensile stretching without fracture (Figs. 4 (c) and (d)).

A fully developed, interconnected fibrous structure was obtained at polymer/sol ratios of 4:1 and 5:1 as shown in Figs. 5 and 6. After firing, this interconnected fiber structure was maintained in the calcium phosphate, although the diameter of the fibers decreased. In general, the fiber diameter decreases with calcination time of up to about 3 to 5 hr. Consequently, the fibers were fired for at least 6 hr. The average diameter of the fibers before and after firing was on the order of 1 μm and 0.8 μm respectively for polymer/sol ratio of 4:1. The corresponding numbers for a ratio of 5:1 are about 1.5 μm and 1 μm respectively.

Hydroxyapatite particles and coatings prepared by various techniques have been used extensively in many biomedical applications [22]. The technique developed by Wu *et al.* [16] which combined the sol-gel process with electrospinning, enabled the development of Hydroxyapatite fibers. In their work, Wu *et al*. [16] were able to produce fibers with diameters between 10 and 30 μm and grain size of about 1 μm. In the present work, it has been demonstrated that by suitably controlling the polymer properties, polymer-sol ratio and the electrospinning conditions, highly interconnected hydroxyapatite fibers with diameters on the order of 0.8 to 2 μm and crystal size of about 30 - 40 nm could be produced by the above mentioned technique. In addition, interconnected porous fibers and highly porous scaffolds can also be produced by controlling the polymer properties as shown in Figs. 6 and 7. Such structures would be highly desirable as bone substitutes or tissue engineering templates.

4.5 CONCLUSIONS

Calcium phosphate fibrous networks with average fiber diameters between 800 nm to 2 μm were produced after calcination of an electrospun PVA/sol mixture. The M_W of the polymer had a significant effect on the final structure obtained after calcination.

At low M_W (- 50,000 g/mol), the addition of the sol disrupted the stable fiber structure that can be formed with the pure polymer. As the M_W is increased to 124,000 g/mol, a stable fiber structure with uniform dispersion of sol particles was obtained. After firing, the polymer phase can be removed and the fibrous structure can be retained in the inorganic phase. Polymer/sol ratios of 4:1 and 5:1 were most effective in producing a fibrous network of calcium phosphate. X-ray diffraction analysis indicated hydroxyapatite to be the dominant inorganic phase remaining after firing. The M_W of the polymer and the polymer/sol ratio can be controlled to obtain highly porous fibers with interconnected pores.

REFERENCES

[1] L. L. HENCH, *J. Am. Ceram. Soc.* **81** (1998) 1705.

[2] A. SLOSARCZYK, E. STOBIERSKA, Z. PASZKIEWICZ and M. GAWLICK, *J. Am. Ceram. Soc.* **79** (1996) 2539.

[3] M. YOSHIMURA, H. SUDA, K. OKAMOTO and K. IOKU, *J. Mater. Sci.* **29** (1994) 3399.

[4] D. LIU, T. TROCZYNSKI and W. J. TSENG, *Biomaterials* **22** (2001) 1721.

[5] M HSIEH, L. PERNG, T. CHIN and H. PERNG, *Biomaterials* **22** (2001) 2601.

[6] O. LYCKFELDT and J. M. F. Ferreira, *J. Eur. Ceram. Soc.* **18** (1998) 131.

[7] P. SEPULVEDA. *Am. Ceram. Soc. Bull.* **76** (1997) 61.

[8] H. R. RAMAY and M. ZHANG, *Biomaterials* **24** (2003) 3293.

[9] C. R. KOTHAPALLI, M. T. SHAW and M. WEI, *Acta Biomaterialia* **1**(2005) 653.

[10] D. TADIC, F. BECKMANN, K. SCHWARZ and M. EPPLE, *Biomaterials* **25** (2004) 3335.

[11] S. R. RAMANAN and R. VENKATESH, *Mater. Lett.* **58** (2004) 3320.

[12] N. YU, C. SHAO, Y. LIU, H. GUAN and X. YANG, *J. Colloid Interface Sci.* **285** (2005) 163.

[13] C.SHAO, H. GUAN, Y. LIU, X. LI and X. YANG, *J. Solid State Chem.* **177** (2004) 2628.

[14] J. YUH, J. C. NINO and W. M. SIGMUND, *Mater. Lett.* **59** (2005) 3645.

[15] S. CHOI, S. LEE, S. S. IM, S. H. KIM and Y. L. JOO, *J. Mater. Sci. Lett.* **22** (2003) 891.

[16] Y. WU and L. L. Hench, *J. Am. Ceram. Soc.* **87** (2004) 1988.

[17] L. H. SPERLING, *Introd. Phys. Polym. Sci.* 2nd Ed. NY: Wiley; 1992.

[18] J. C. J. F. TACX, H. M. SCHOFFELEER, A. G. M. BRANDS and L. TEUWEN, *Polymer* **41** (2000) 947.

[19] A. KOSKI and S. SHIVKUMAR, *Mater. Lett.* **58** (2004) 493.

[20] B. D. CULLITY, and S. R. STOCK, Elements of X-Ray diffraction, 3rd edition, New Jersy: Prentice-Hall, Inc. 2001

[21] X. ZONG, K. KIM, D. FANG, S. RAN, B. S. HSIAO and B. CHU, *Polymer* **43** (2002) 4403.

[22] W. SIGMUND, J. YUH, H. PARK, V. MANEERATANA, G. PYRIGIOTAKIS, A. DAGA, J. TAYLOR and J. C. NINO, *J. Am. Ceram. Soc.* **89** (2006) 395.

LIST OF FIGURES

TABLE 1 *Materials used in this investigation and the corresponding suppliers. The concentration of the polymer (c) used in the solution is also shown. Experiments were conducted for (polymer solution)/(inorganic sol) ratios of 1:5, 1:3, 1:1, 3:1 and 5:1 respectively. All the raw materials were obtained from Aldrich Chemical Company, Milwaukee, WI.*

Materials	*Relevant Properties*	*c (wt %)*
TEP	98%	
$Ca(NO_3)_2 \cdot 4H_2O$	99%	
PVA	50,000 – 85,000g/mol, 97% hydrolyzed	15.5
PVA	124,000 – 186,000g/mol, 99+% hydrolyzed	10.7

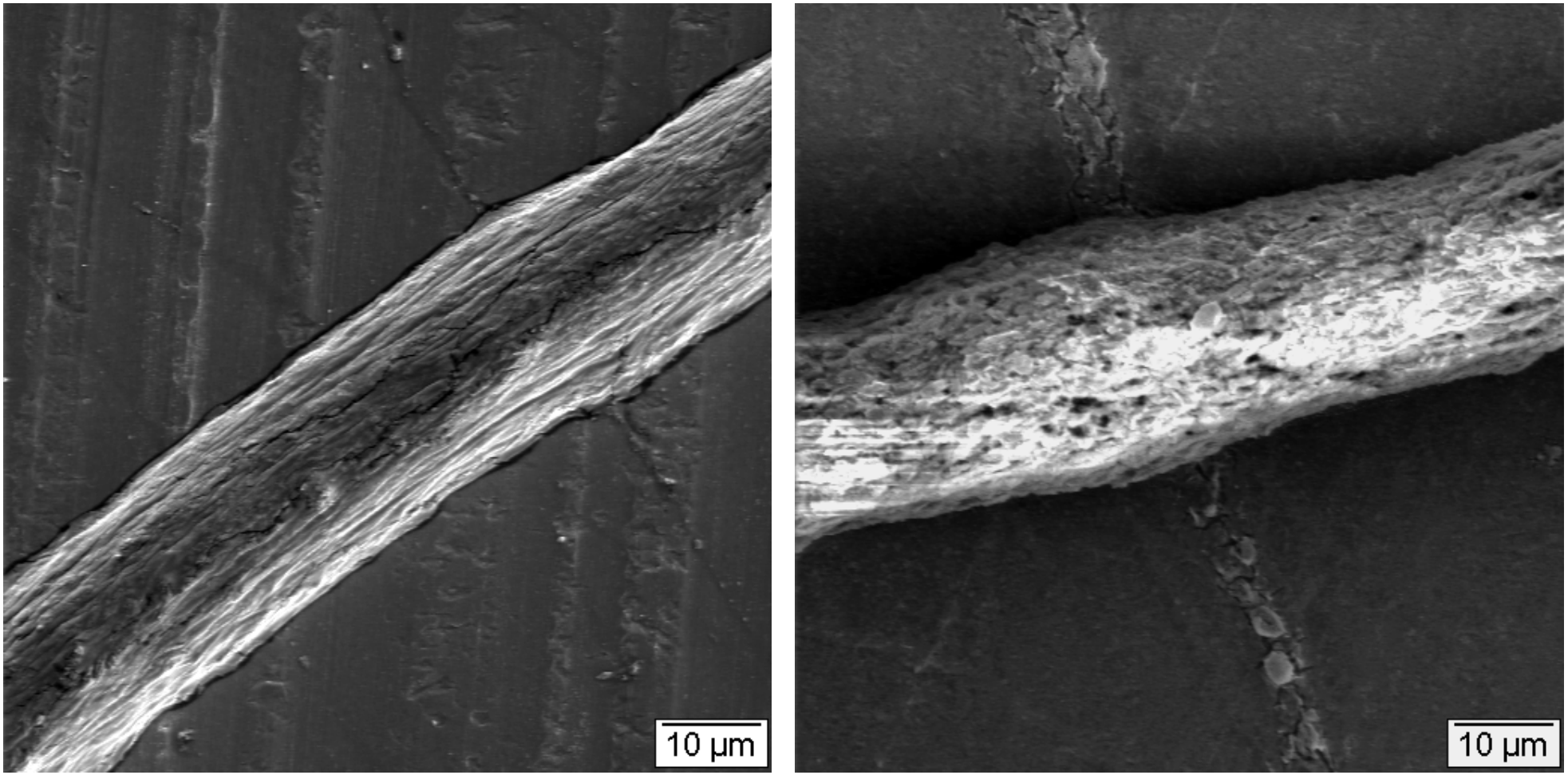

(a) **(b)**

Figure 1 *Photographs showing (a) electrospun fiber and (b) electrospun fiber calcined at 600 ^{o}C for 6 hr. (M_W = 50,000 - 85,000 g/mol; PVA/sol volume ratio =3:1)*

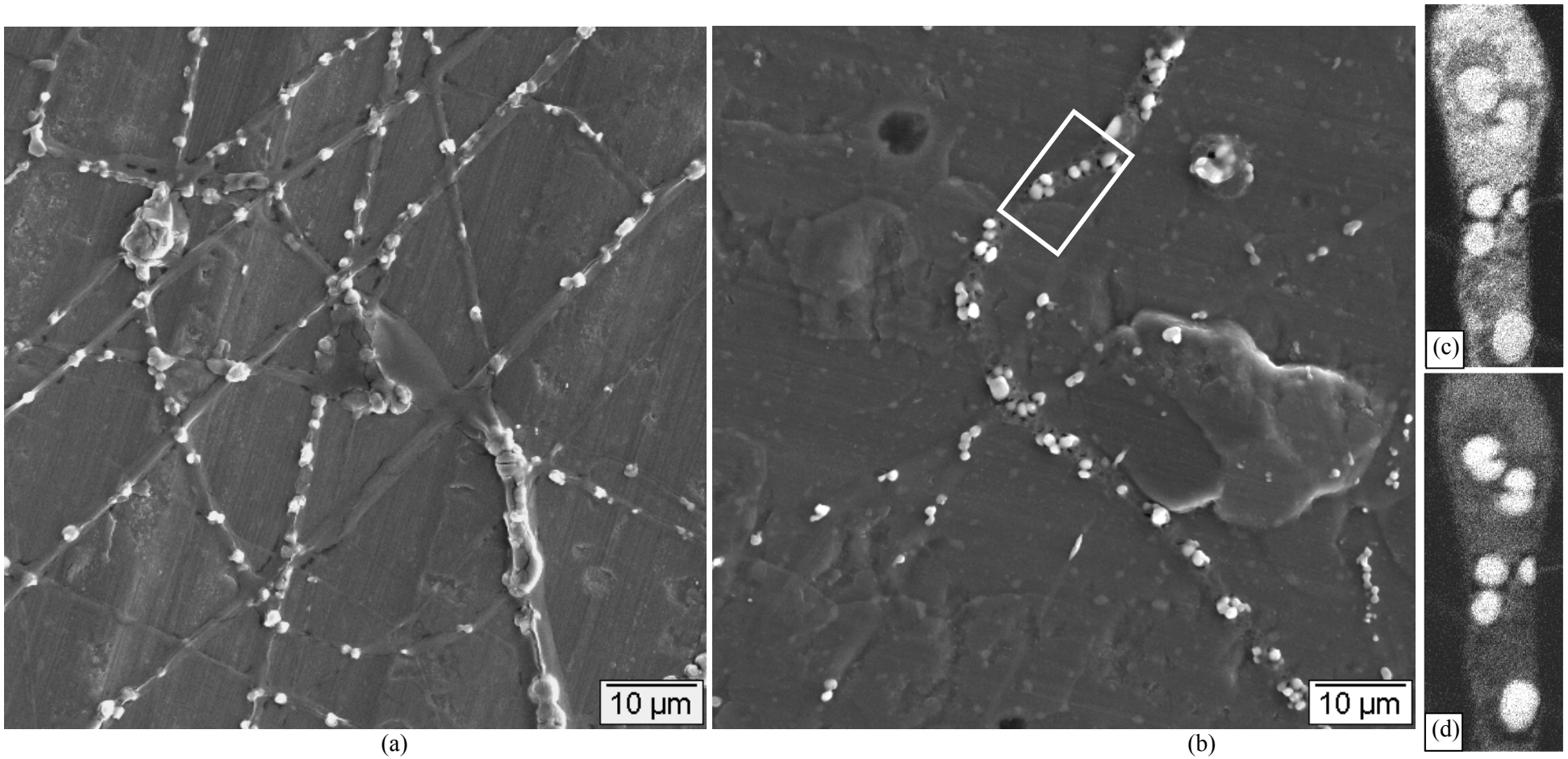

Figure 2 *Photographs showing (a) electrospun fibrous structure and (b) fibrous structure after 600 ^{o}C 6 hr firing. The insets (c) and (d) show the elemental maps of the highlighted area of Calcium (c) and Phosphorous (d) by EDX analysis. (PVA, M_W = 124,000 - 186,000 g/mol, PVA/sol volume ratio =3:1).*

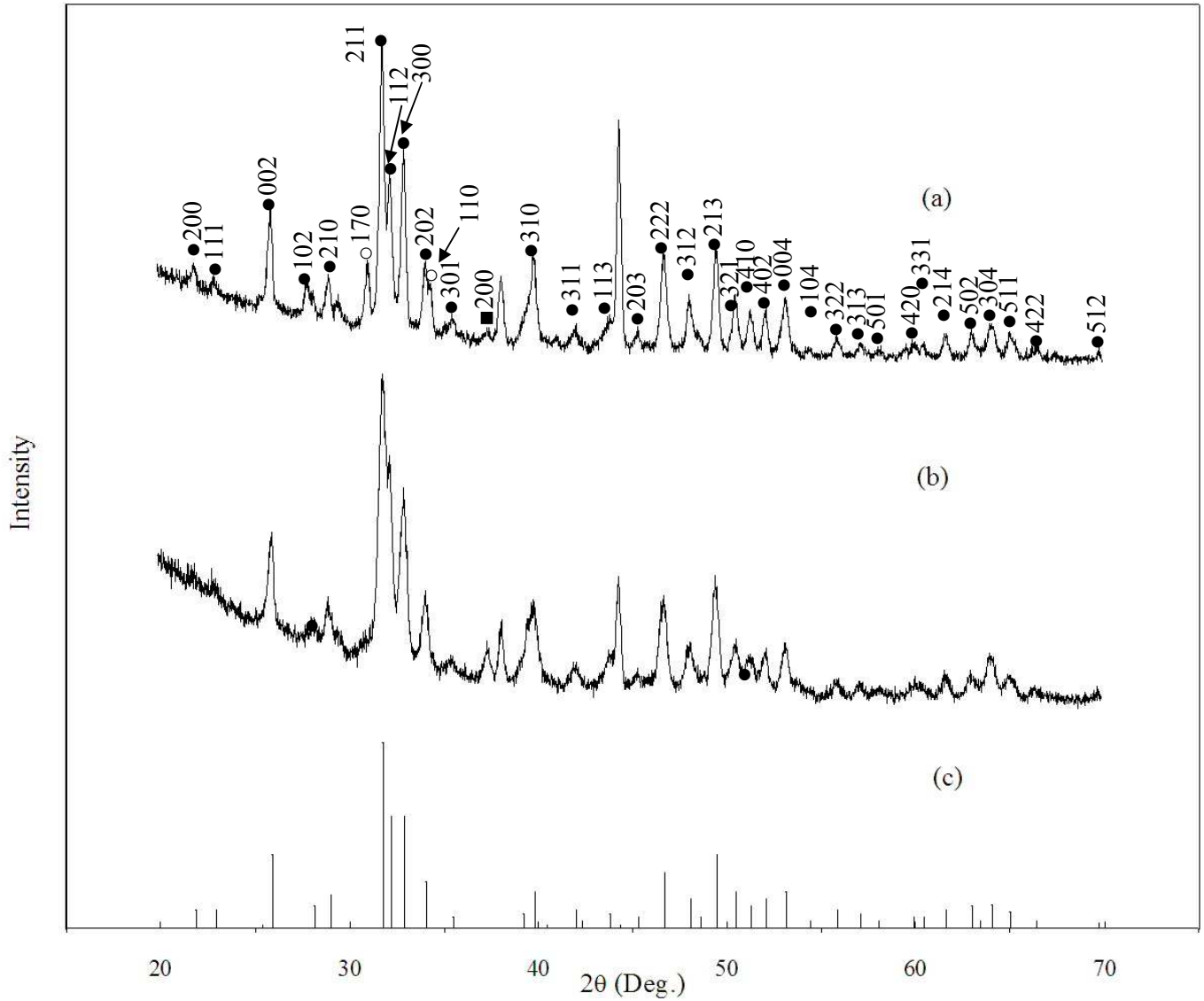

Figure 3 *X-ray diffraction pattern of a) pure sol calcined at 600°C for 6 hr and b) polymer/sol mixture (M_W = 124000-186,000 g/mol) calcined at 600 °C for 6 hr. The peaks for hydroxyapatite (●), CaO (■) and β-tricalcium phosphate (○) are indicated. The corresponding diffraction pattern from the JCPDS file for pure Hydroxyapatite is also presented [JCPDS file # 09-0432].*

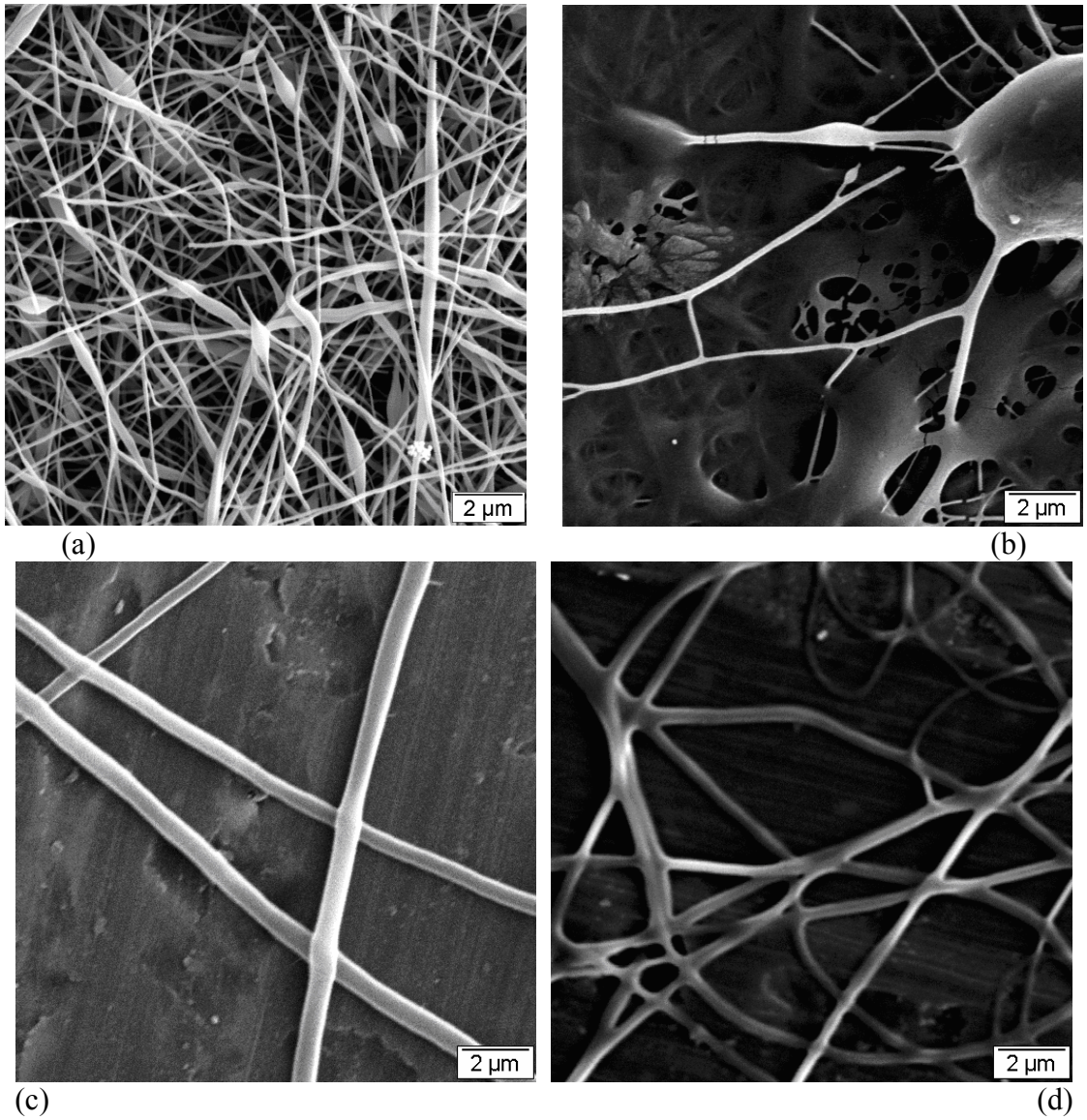

Figure 4 *Photographs showing the effects of sol addition to the polymer solution on the structure in the electro spun polymer for two different M_W. (a) Pure PVA, M_W = 50,000 - 85,000 g/mol, (b) PVA/sol, M_W = 50,000 - 85,000 g/mol, (c) Pure PVA, M_W = 124,000 - 186,000 g/mol and (d) PVA/sol, M_W = 124,000 - 186,000 g/mol. The polymer solution to sol volume ratio was maintained at 5:1 for samples in (b) and (d).*

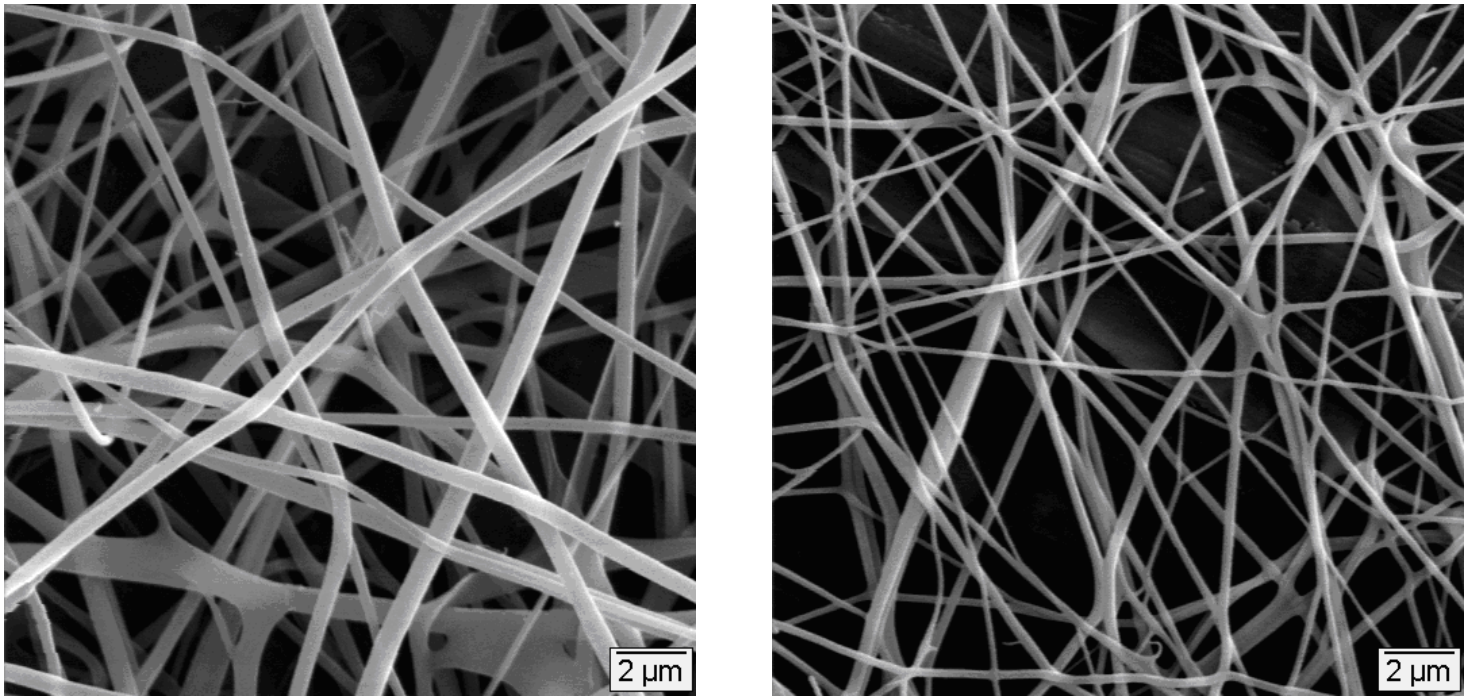

(a) **(b)**

Figure 5 *Photographs of (a) electrospun fibrous structure and (b) the structure after the electrospun sample was fired at 600 ^{o}C for 6 hr. (M_W = 124,000 - 186,000 g/mol, PVA/sol volume ratio =5:1)*

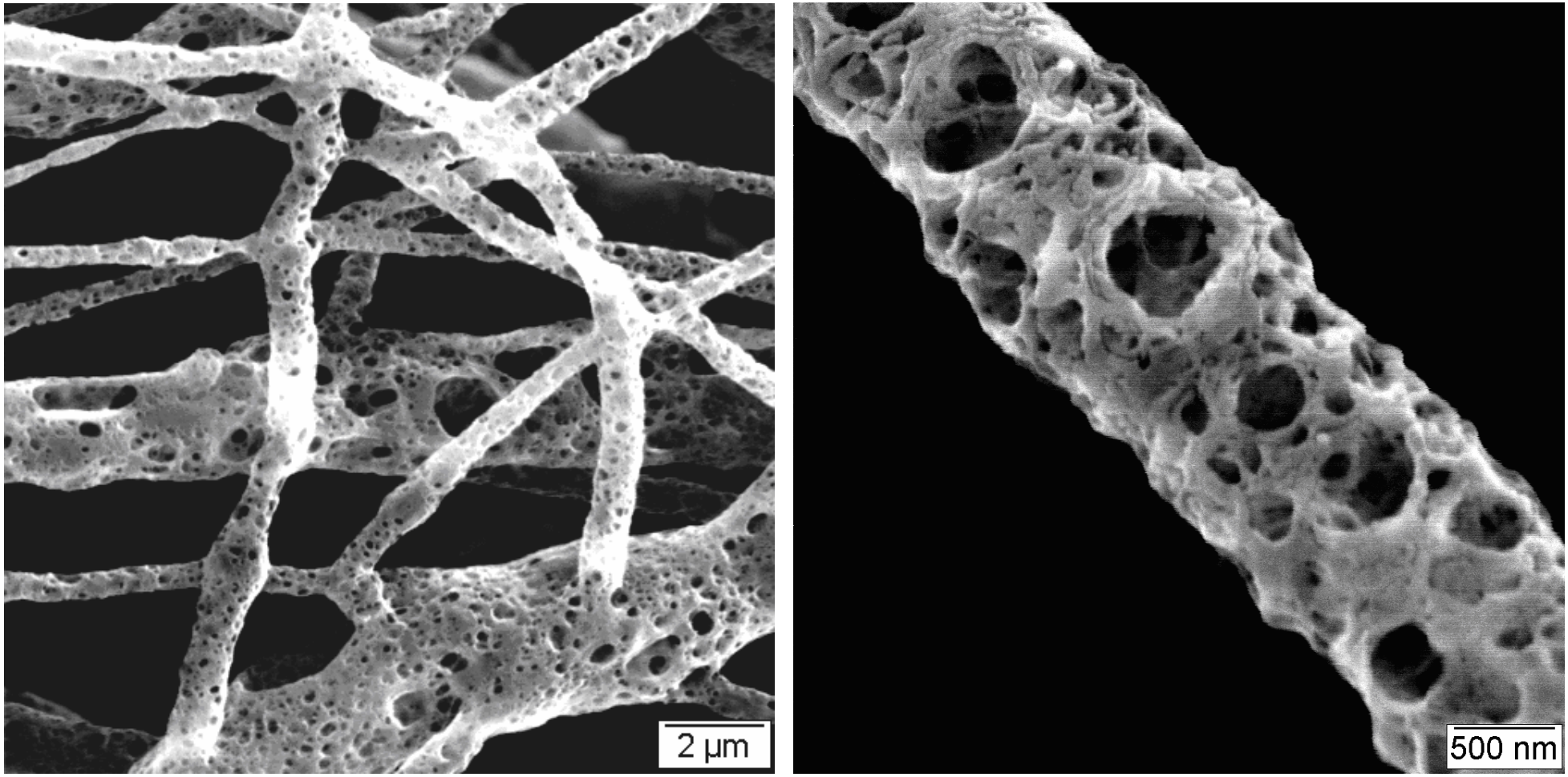

(a) (b)

Figure 6 *Photograph showing porous interconnected fibers after firing at 600 ^{o}C for 6 hr (a). A high magnification photograph of a single fiber is shown in (b). (PVA/sol volume ratio = 4 :1, M_W = 124,000 - 186,000 g/mol)*

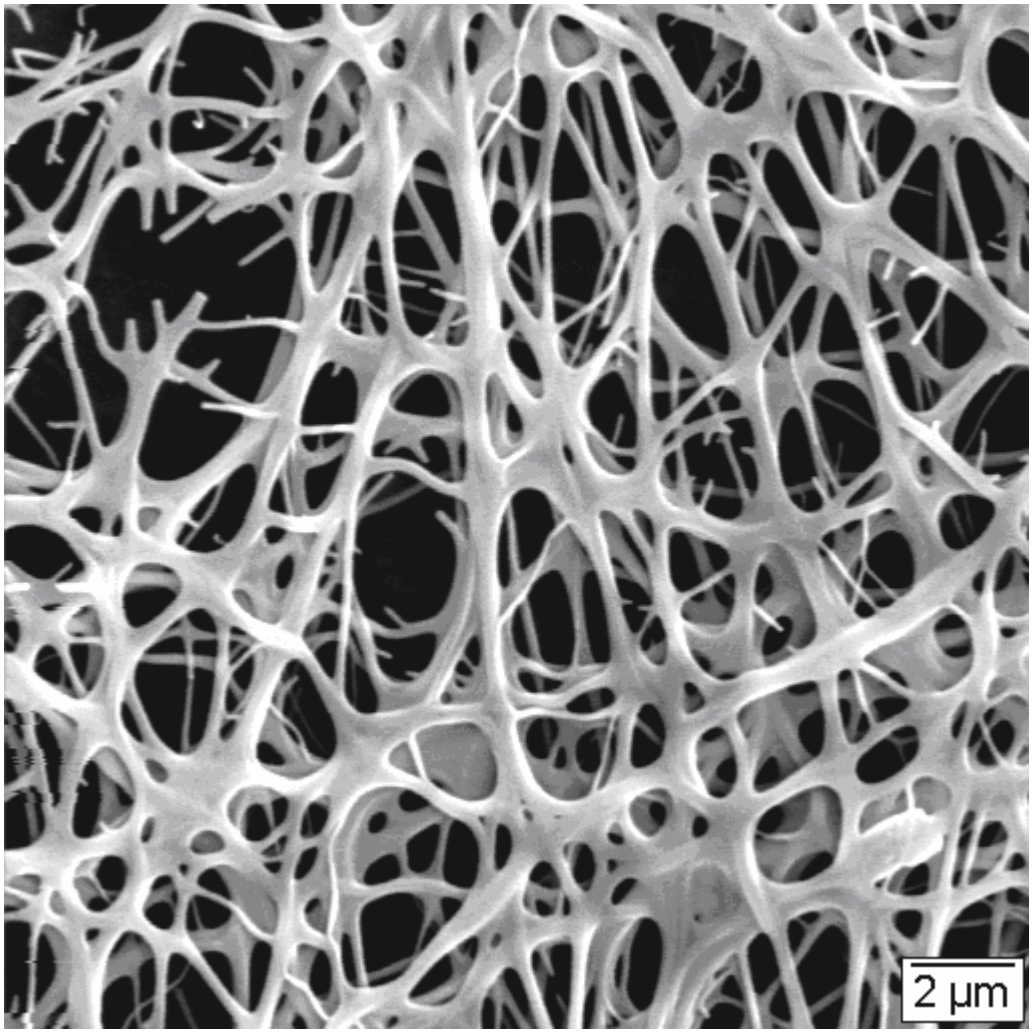

Figure 7 *Photograph showing an interconnected network of fibers. The electrospun polymer was fired at 600 ℃ for 6 hr. (PVA/sol volume ratio =4 :1, M_W = 50,000 - 85,000 g/mol)*

5. EFFECT OF POLYMER MOLECULAR WEIGHT ON THE INORGANIC FIBROUS NETWORK

5.1 Abstract

PVA with three different molecular weights were electrospun with a calcium phosphate based sol to produce calcium phosphate fibrous structures. The average molecular weight was varied from 40,500 g/mol to 155,000 g/mol. The volume fraction of the sol added to the polymer solution was varied from 0% to 100%. The electrospun structures were calcined at 600^{o}C for 6 hr. The calcined structures were examined by X-Ray diffraction (XRD) and Scanning Electron Microscopy (SEM). The results indicate the morphologies of the electrospun patterns are depend strongly on the polymer molecular weight (M_W) and sol volume fraction. At molecular weight of 67,500 g/mol and 155,000 g/mol, a completely fibrous structure was obtained after electrospinning. This fibrous structure was retained after calcination. Average fiber diameters were on the order of 200 nm and 800 nm for molecular weight of 67,500 g/mol and 155,000 g/mol, respectively. When M_W = 40,500 g/mol, a bead-on-string structure was obtained after electrospinning, which was retained after calcination. The calcined structure consists predominantly of HA crystals with average size on the order of 10 – 30 nm.

5.2 Introduction

Bioceramic scaffolds have the advantage of chemical similarities to natural hard tissue [2]. They are designed to be used in orthopedic and dental applications because of their biocompatibility characteristics. Hydroxyapatite ($Ca_{10}(PO_4)_6(OH)_2$, HA) is the main mineral content of teeth and bone and hence is the most appropriate synthetic bioceramic for hard tissue replacement and repair. In addition, it also has excellent biocompatibility with soft tissues like skin and mussel [55]. Therefore, HA scaffolds can be promising materials for various applications. These scaffolds can either be used directly as the implant materials or be incorporated as a reinforcement phase for polymer/ceramic biodegradable bone substitutes [3]. In recent years, HA containing implants have been investigated as vehicles for drug delivery [2].

Electrospinning has been developed as a simple and versatile method for producing fibers. Recently, this technique has been extensively used for producing ceramic fibers combined with sol-gel method. Typically, an inorganic precursor is produced by the sol-gel method. This sol is mixed with a suitable polymer solution and electrospun at a high voltage. The electrospun structure is calcined at temperatures on the order of 600^{o}C. The polymer is removed and the crystallization of the ceramic is also accomplished during the calcination procedure [35].

Among the studies of ceramic electrospinning to date, most of the reports have been focused on the fabrication and the ceramic property evolution. Few studies have been dedicated to the effect of polymer and polymer solution properties. A preliminary investigation has shown that polymer

molecular weight and concentration may have a strong influence on the morphology of the inorganic structure [63]. In this investigation, the effects of molecular weight and the sol volume fraction in the mixture on the electrospun structure have been investigated. The effects of these variables on the crystallization in the apatitic phase have been studied.

5.3 Materials and Method

5.3.1 Materials

Triethyl phosphite (TEP, Aldrich, USA) and calcium nitrate tetrahydrate ($Ca(NO_3)_2 \cdot 4H_2O$, Aldrich, USA) were used as the raw materials for preparing the inorganic sol. PVA with various weight average molecular weights (M_W) was obtained from Aldrich Chemical Company, Milwaukee, WI. Distilled water was used as the solvent.

5.3.2 Preparation of the Sol

The inorganic sol was prepared by sol-gel routine described previously [33]. The flow chart in Fig. 13 shows the experimental procedure for producing the transparent sol. Appropriate amounts (11.9 g) of calcium nitrate tetrahydrate (to obtain a Ca/P ratio of 1.67) were dissolved in 10 mL of distilled water. About 5.2 mL of triethyl phosphite was hydrolyzed with 10 mL of distilled water. The nitrate solution was added dropwise into the hydrolyzed phosphate solution. The resulting mixture was stirred vigorously for 2 hr in an aqueous environment and

aged at different temperatures for different time as shown in Table 3. The sol used for preparing the electrospun precursor was aged at 80°C for 24 hr. A transparent sol was obtained after the aging treatment.

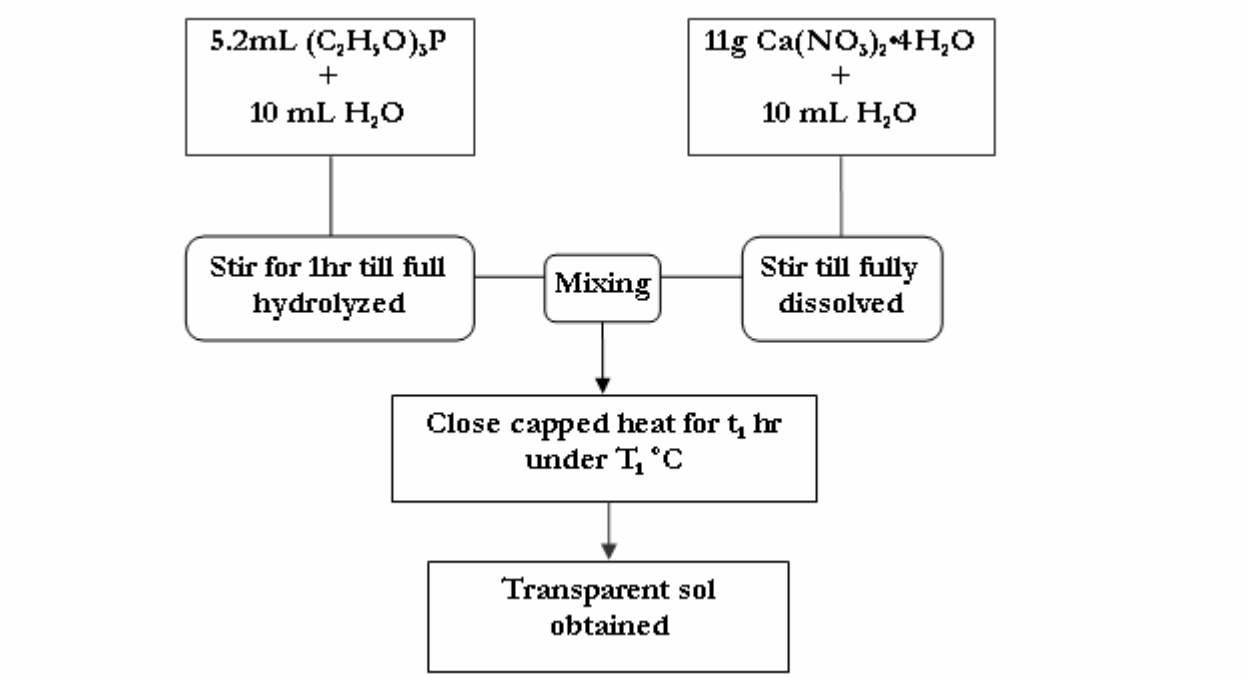

Fig. 13 Flow chart showing the experimental procedure for preparing the sol.

Table 3 Experimental Conditions used during the production of the sol (a) and the inorganic powder (b).

Aging Temperature, T_1(°C)	70	80
Aging time, t_1(hr)	24	
Calcination Temperature, T_2(°C)	700	
Calcination time, t_2(hr)	2	

(a)

Aging Temperature, T_1(°C)	70									
Aging time, t_1(hr)	36									
Calcination Temperature, T_2(°C)	300	400	500	600	700					800
Calcination time, t_2(hr)	0.5	0.5	0.5	0.5	0.5	2	3	4	5	0.5

(b)

5.3.3 Preparation of the polymer solution

Appropriate amounts of PVA were dissolved in distilled water. The dissolution was conducted in a water bath at 80^{o}C, with constant stirring for at least 2 hr to ensure complete dissolution.

5.3.4 Preparation of the polymer-sol mixtures

The electrospinning precursor was prepared by mixing the sol and the polymer solutions at room temperature. The volumetric ratio between the PVA solution and the inorganic sol was varied between 1:5 and 5:1 corresponding to sol volume fraction between 83.3vol% and 16.7vol%. The mixture was then sealed and vigorous stirring was continued for at least 8 hr at 25^{o}C. After this, the stirring was stopped to facilitate the removal of gas bubbles. The specific values of concentration used with each molecular weight are also summarized in Table 4.

Table 4 Weight average molecular weight (M_W), %hydrolyzation and concentration (wt %) of PVA used to prepare the inorganic-organic hybrid mixture.

M_W (g/mol)	% Hydrolyzation	Concentration (wt %)
40,500	98-99	20
67,500	97	15
155,000	99+	10

5.3.5 Viscosity Measurements

The viscosity of the pure sol, pure PVA solution, and PVA/sol mixtures at 25°C was measured using a digital rheometer (Brookfield Model DV III). Approximately 0.5 mL of the mixture was placed in the center of the small sample adapter. This sample was premixed for 10 min at the 100% Torque to ensure thorough contact between the solution and the cone-plate. At least 15 different shear rates were used for each measurement. The shear rate was varied between $0.1s^{-1}$ and $450s^{-1}$. The operation time was adjusted to be 3 min for each shear rate. At the end of the operation time, viscosity data were collected instantaneously. The zero shear rate viscosity is calculated based on power law equation:

$$\eta = A\gamma^n \tag{6}$$

5.3.6 Electrospinning of the Mixture

The electrospinning apparatus consisted of a 1 mL syringe, equipped with an 18-gauge (Outer diameter = 1.27 mm, 52 mm long) stainless steel needle that were mounted horizontally in a syringe pump as shown in Fig. 14. A potential of 20 to 30 kV was applied to the needle immediately after a pendant drop formed at the tip of the needle. The collector plate was covered with aluminum foil, weighed in advance, and positioned at a distance of 10 cm from the needle.

A high speed camera (Phantom V.5.1., Vision Research) equipped with Nikon 150 mm lens was used to monitor the transit of different solutions from the capillary at a rate of 2000 frames per

second with exposure time of 259 μs. The images were extracted and analyzed with *CineView606* supplied by Vision Research.

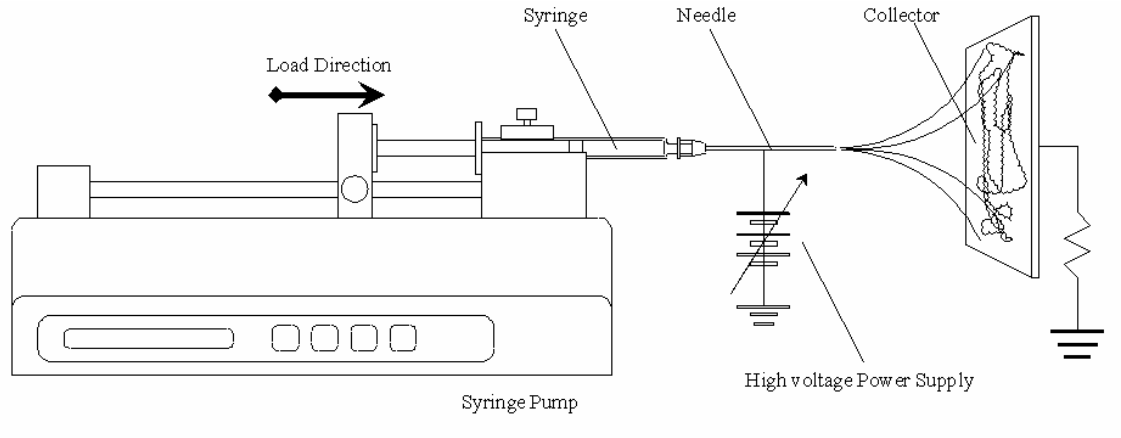

Fig. 14 Schematic illustration of the experimental set-up.

The PVA/Sol mixtures obtained after electrospinning were dried at room temperature for at least 8 hr and then weighed. Some of the as-spun samples were freeze dried. The freeze drying was conducted at -45^{o}C, 0.067 kPa for approximately 2 hr. Subsequently, the vacuum was reduced to less than 0.0267 kPa. The samples were gradually warmed up to 0^{o}C. After holding for about 18 hr, the samples were gradually warmed up to 20^{o}C until they were taken out.

5.3.7 Calcination

The sol was dried at 80^{o}C for 24 hr to drive off all the solvent. A white gel was obtained after drying. The gel was calcined at temperatures between 300 - 800^{o}C for various times. A white powder was generally obtained after calcination. The times and temperatures used are summarized in *Table 3(b).* The dried electrospun hybrid samples were calcined at 600^{o}C for 6 hr.

After calcination, the sample was weighed again and the weight loss during calcination was calculated. The freeze dried samples were also subjected to the same calcination procedure. The calcination procedures for the electrospun hybrid mixture are shown in Figs. 15 and 16.

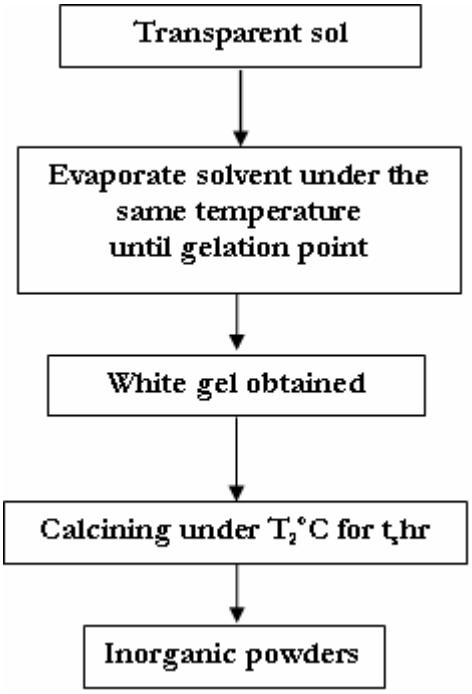

Fig. 15 Flow chart showing the experimental procedure for producing the inorganic powder.

5.3.8 Structural Characterization

The white powder obtained after calcination was analyzed by X-Ray diffraction (XRD) (Rigaku) with Cu *K-α* radiation. Also XRD analysis was conducted on the small sample scraped off from the calcined electrospun sample. The diffraction data were analyzed with JADE software. The electrospun samples were sputter coated with gold-palladium and examined in JSM-840 scanning electron microscope (SEM). The SEM images were analyzed with *Analysis* image

analysis software provided by *Softimaging Systems* to obtain data on the fiber diameter. For fiber diameter measurement, more than 50 fibers were examined under each condition.

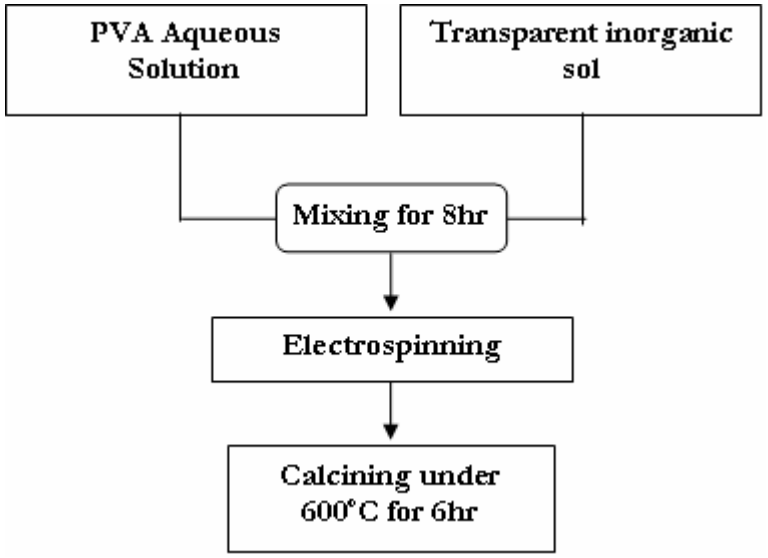

Fig. 16 Flow chart showing the experimental procedure for fabricating the inorganic fiber.

5.4 RESULTS AND DISCUSSION

5.4.1 Preparation of the sol

A colorless sol with a zero shear viscosity of 6mPa·s was obtained after the aging process. When this sol was calcined, the structure consists predominantly of HA and minor phases, such as β-tricalcium phosphate and CaO, in small fractions [12]. It has been reported that the aging time and temperature are critical in the formation of HA [33]. The effect of aging temperature and aging time are shown in Fig.17 and Fig. 18, respectively.

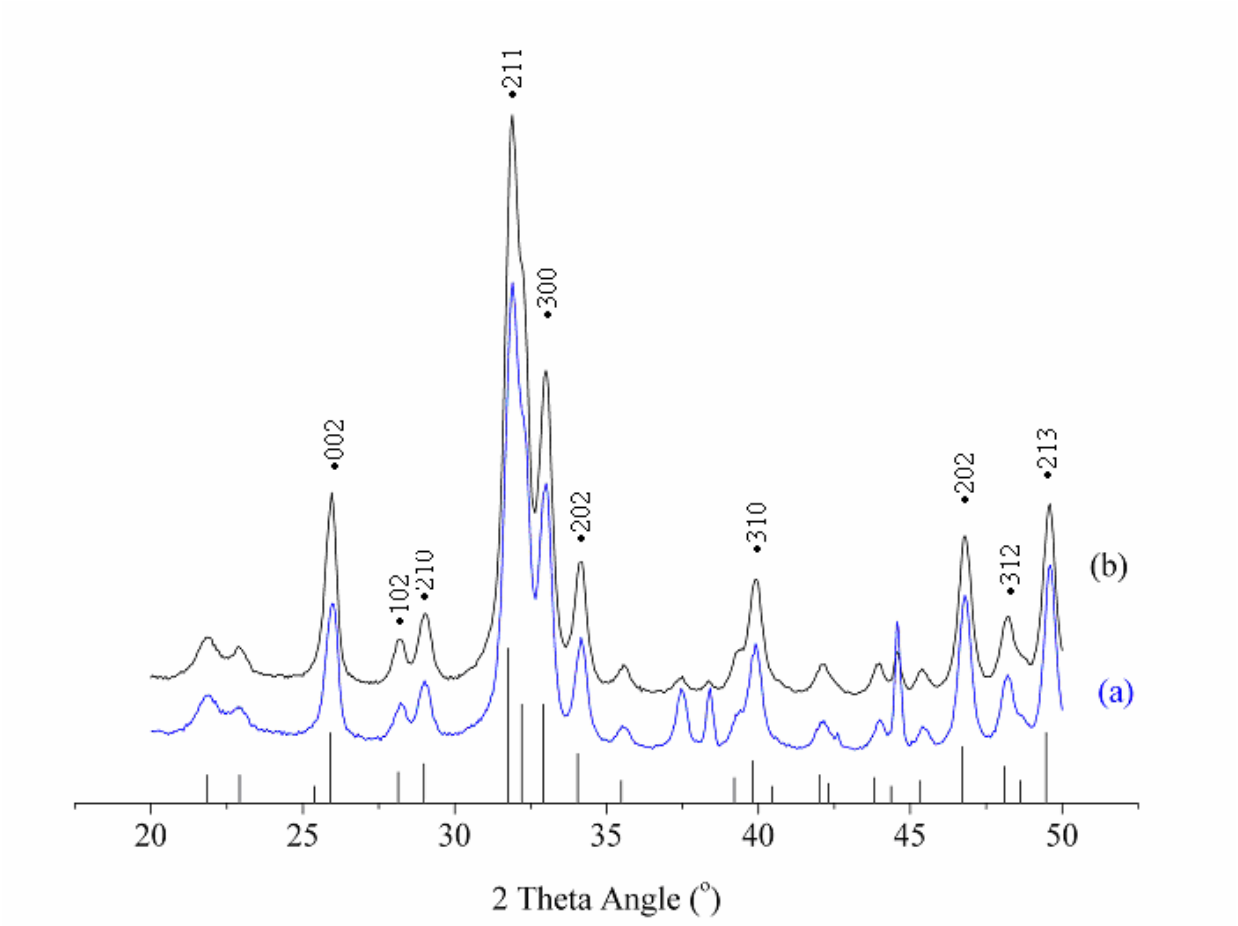

Fig. 17 X-ray diffraction patterns for sols aged at (a) 70°C and (b) 80°C. After aging for 24 hr at the preceding temperatures, the sol was calcined at 700°C for 2 hr. The primary diffraction peaks for hydroxyapatite (●) are indicated.

It can be observed that the intensity of the characteristic peaks corresponding to HA phase in samples aged at 80°C is more pronounced than the samples aged at 70°C. It has been reported by several investigators researchers that higher aging temperatures favor of the formation of HA [12]. The aging time did not have a significant effect on the formation of HA (Fig. 18). In this case, there are no obvious distinctions between the characteristic peaks of HA phase within the two samples. The characteristic peaks at $2\theta = 29.8\text{-}31.1°$ indicate the presence of β- tricalcium

phosphate (β-TCP) in the samples aged for 36 hr. This phenomenon is consistent with the data of Chai *et al*. [20], who reported that there is a trend towards the formation of β-TCP when a longer aging time is used. Thus, any aging time longer than 36 hr may not be desirable for the formation of HA.

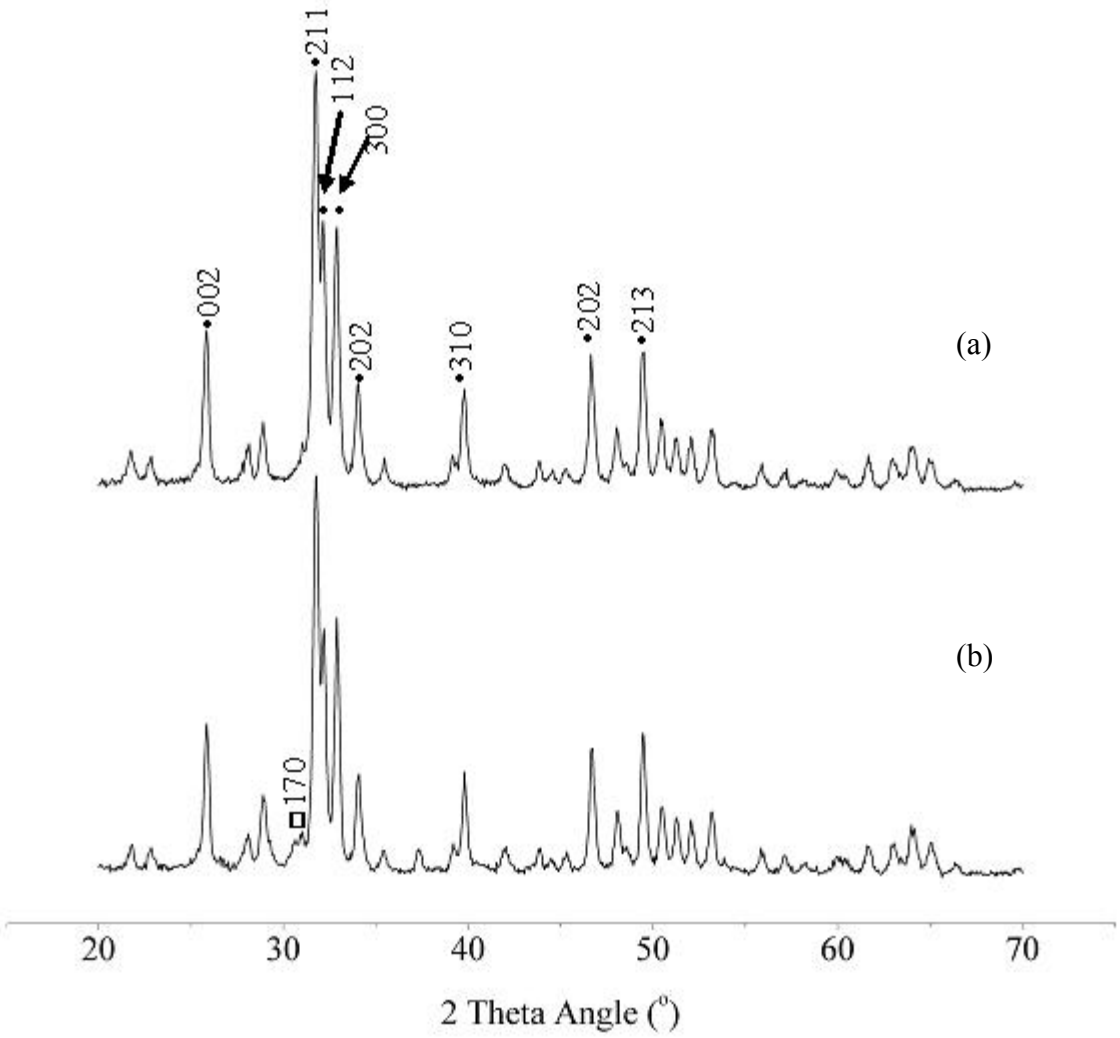

Fig.18 XRD pattern of 70°C aged sol for (a) 24 hr and (b) 36 hr. The samples are calcined at 700°C for 2 hr. The primary diffraction peaks for hydroxyapatite (●) and β-tricalcium phosphate (□) are indicated.

Liu *et al.* [12] reported that a minimum 8 hr aging is necessary to obtain HA and prevent the formation of the secondary phase, CaO. They also concluded that the fraction of HA increases and impurity phases, such as CaO, $Ca_2P_2O_7$, $Ca_3(PO_4)_2$, gradually disappear with increasing aging time. In the XRD patterns of both samples (Fig. 18), there is no evident peak corresponding to the CaO phase. Thus, the formation of the CaO phase can be minimized by the aging process in this investigation.

5.4.2 Calcination of the gel

The sol was heat treated at 80^{o}C to drive off the solvent and form a white gel. During this procedure, a weight loss about 50wt% was observed. This weight loss was mainly from the loss of the absorbed solvent (water and alcohol). The dried gel was calcined at various temperatures for various times. Upon calcination, an additional 40wt% weight loss was observed. This is primarily due to the decomposition of the nitrate salt and the loss of the combined water. The XRD patterns of the gel prepared from treating the sol at 70^{o}C for 36 hr followed by calcination for 0.5 hr at various temperatures are shown in Fig. 19. It can be seen that a highly crystalline form of HA is observed upon calcination. The characteristic peaks of HA phase were first observed in the sample calcined at 500^{o}C. This result is consistent with the data of Chai *et al.* [14] and Lopatin *et al.* [22], who reported that the temperature to form crystallized hydroxyapatite is between 420^{o}C and 460^{o}C. Some of the characteristic peaks in Fig. 19 also correspond to the secondary phase – β-tricalcium phosphate. This phase starts to become distinguishable in the diffraction pattern of samples calcined at 800^{o}C. Similar results have been

reported by several investigators, which suggest that the formation temperature of β-tricalcium phosphate is between 750°C - 800°C [14].

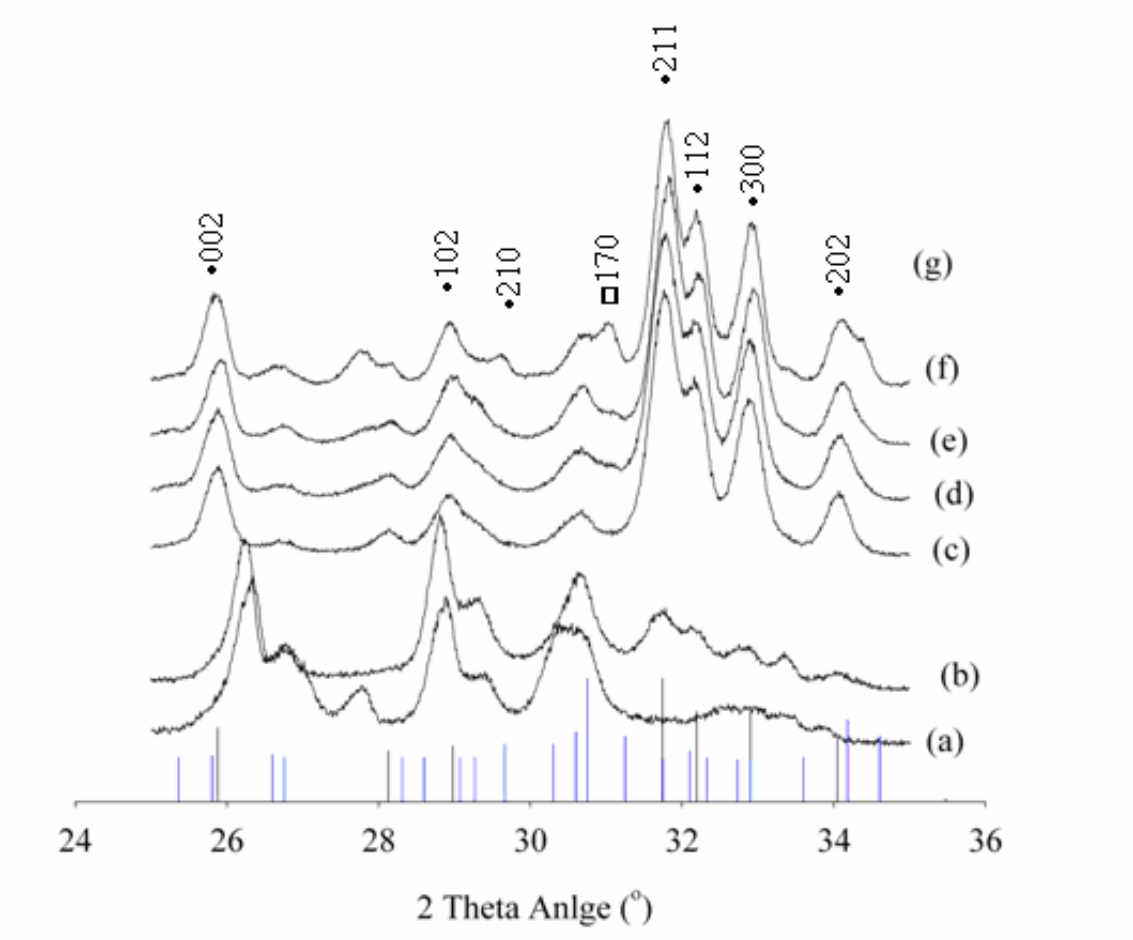

Fig.19 X-Ray diffraction pattern of the gel calcined at different temperatures for 0.5hr (a) 300°C, (b) 400°C, (c) 500°C, (d) 600°C (e) 700°C (f) 800°C. The primary diffraction peaks for hydroxyapatite (●) and β-tricalcium phosphate (□) are indicated.

The crystal size was calculated based on the X-ray diffraction pattern according to the Scherrer equation [34] to further investigate the influence of the calcination temperature.

$$B = \frac{0.9\lambda}{t\cos\theta} \quad \textbf{(1)}$$

where *B* equals to FWHM (full width at half maximum) of the broadened diffraction line on the 2θ scale, which, in this investigation, is the reflection of (002) and (211) planes, λ is the wavelength for Cu-Kα (λ =0.15418 nm) and *t* is the diameter of the crystallites**.** The average value was taken as the final value of the crystal size and is typically between 20 and 40 nm. The crystal size data as a function of calcination temperature are plotted in Fig. 20.

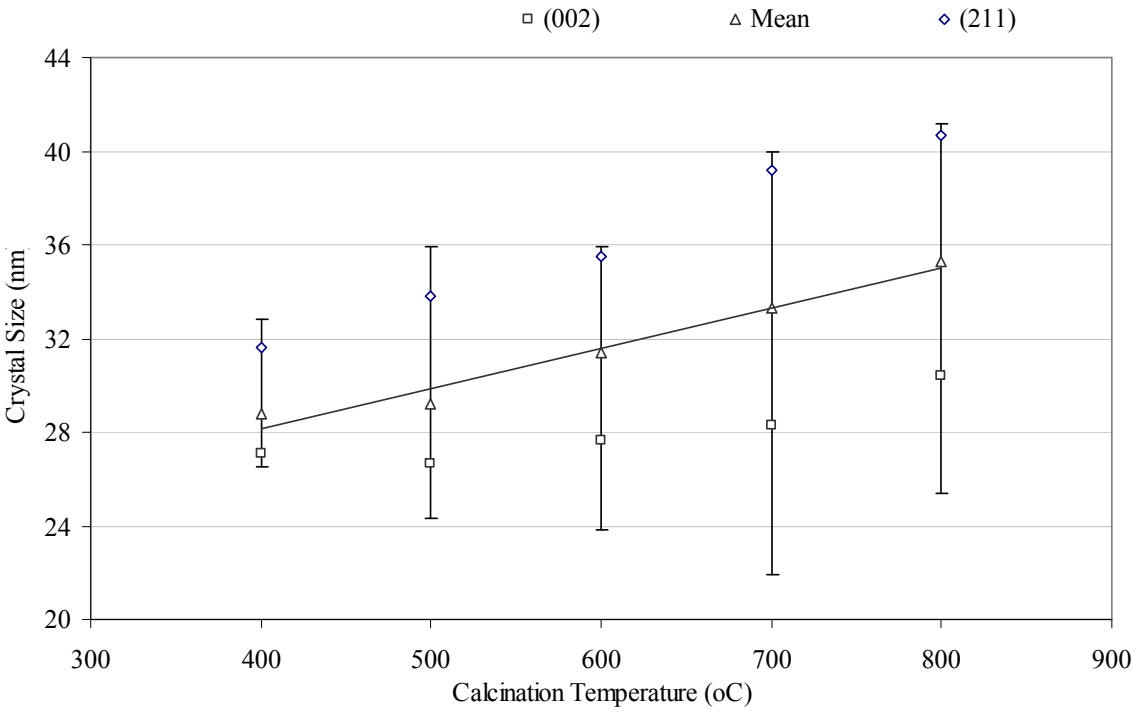

Fig. 20 Crystal size as a function of calcination temperature.

It is observed that the crystal size increases with increasing calcination temperature. This is consistent with the data of Liu *et al.* [33] who studied line-breadth of the (002) peak at 2θ=25.83^{o} of the apatitic powder for gels calcined at different temperatures. The half-intensity width of the (002) peak decreased gradually with a corresponding improvement in the sharpness of the major

peaks as the temperature increased from 350°C to 800°C. This observation indicates an increase in crystallite size or improved crystal perfection of the calcined HA powders. On the other hand, an increase in the crystal size might cause the coarsening of the final powder. Thus, high temperature calcination may favor of the formation of a secondary phase as well as the increase of the crystal size, which is not desirable in some of the applications.

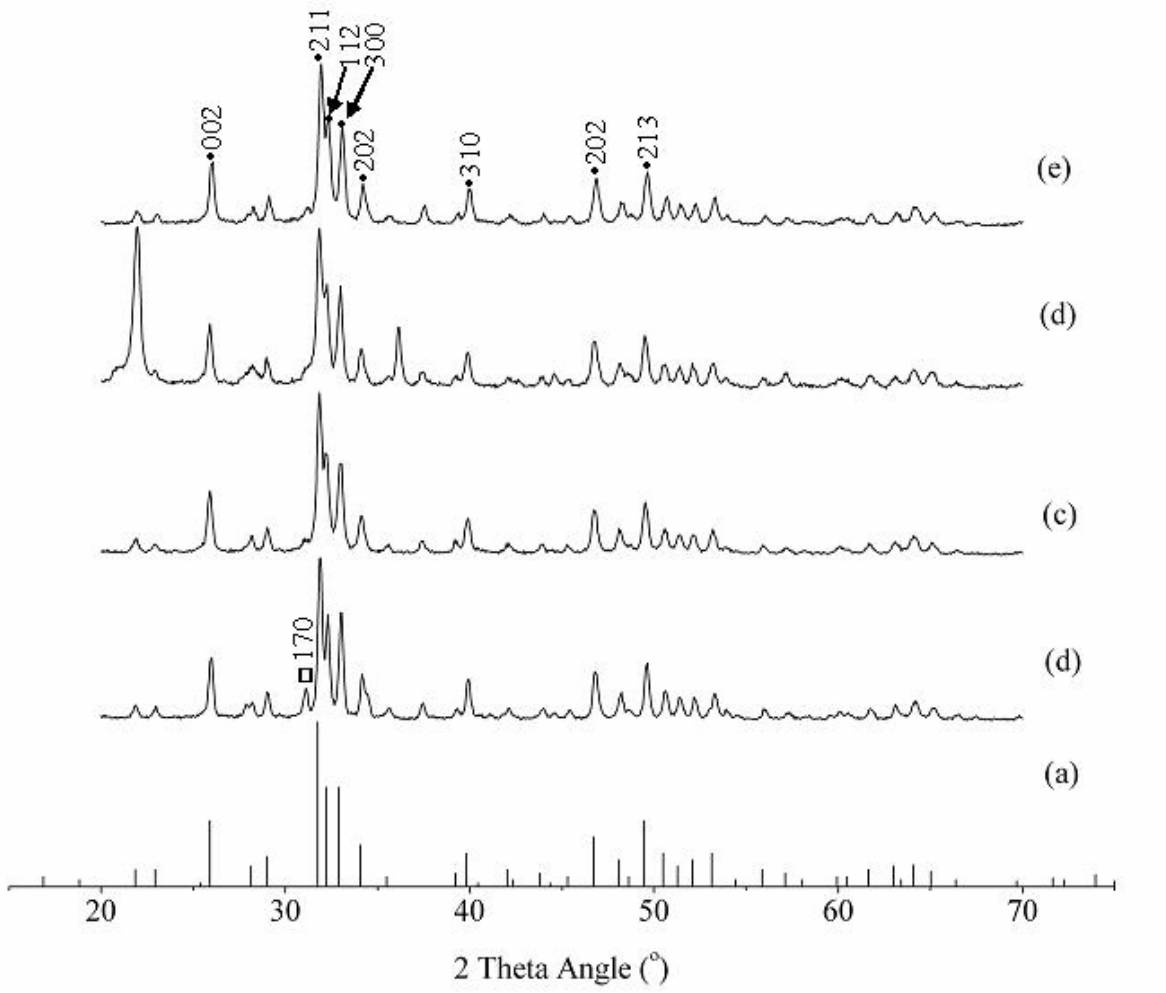

Fig. 21 *X-ray data of 700°C calcined 70°C 24 hr Samples: (b) 700°C calcining for 2hr; (c) 700°C calcining for 3hr; (d) 700°C calcining for 4hr; (e) 700°C calcining for 5hr. The standard hydroxyapatite diffraction pattern (JCPDS file #09-0432) (a) is also shown at the bottom of the figure. The primary diffraction peaks for hydroxyapatite (●) and β-tricalcium phosphate (□) are indicated.*

The XRD patterns of samples calcined at 700°C for different time are shown in Fig. 21 followed by the relevant crystal size data shown in Fig. 22. A slight increase of the crystal size was observed with increasing calcination time, while no signification differences were observed in the XRD patterns. A rapid rate of crystallization was observed by Lopatin *et al.* [22] for the amorphous calcium phosphate to HA transformation. They reported 80% crystalline HA can be obtained within 200 s at a temperature as low as 460°C. Hence, longer calcination time might not favor increased crystallization, but may lead to coarsening of the crystals as indicated above.

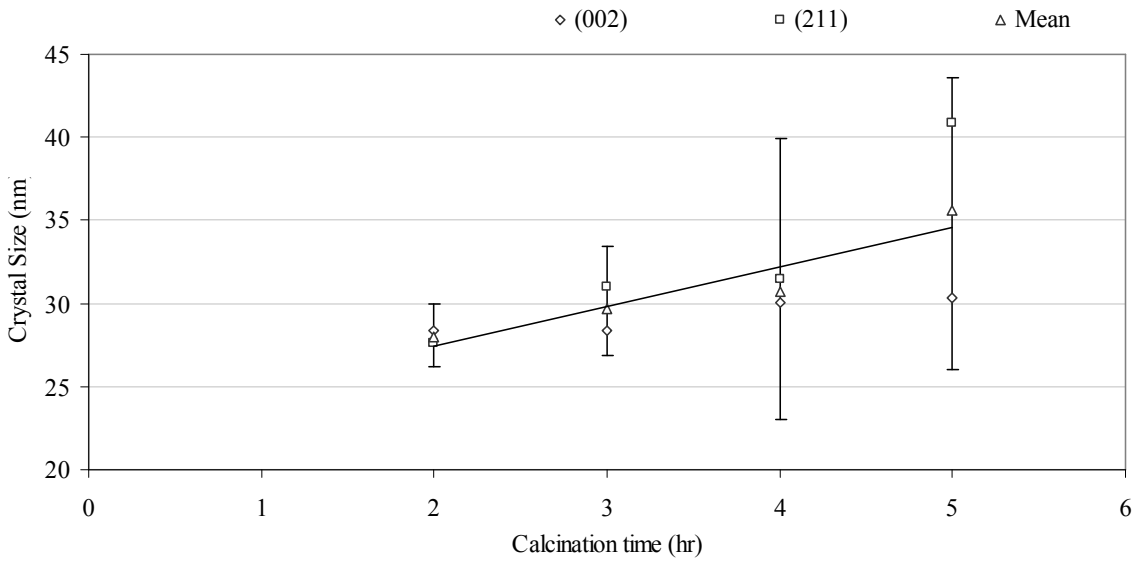

Fig. 22 Crystal size as a function of calcination time.

5.4.3 Electrospinning of the sol

After electrospinning the pure sol, a transparent coating can be observed on the aluminum foil. This indicates no gelation occurred during the electrospinning procedure. A white gel will not form until the sample was dried in room temperature. Gelation occurs when adequate solvent is

driven off from the sol [33]. By maximizing the surface area, electrospinning accelerates the evaporation of the solvent, in other words, improves the gelation. The weight loss of the as-spun sol after drying is about 63wt% upon calcination. This weight loss is highly dependent on the amount of solvent contained in the sol/gel. Thus, the value may vary slightly because of the different drying times and temperatures used. The SEM pictures of as-spun sol and calcined sol are shown in *Figs. 23 (a) and (b)*. The detailed results are discussed in the following chapter.

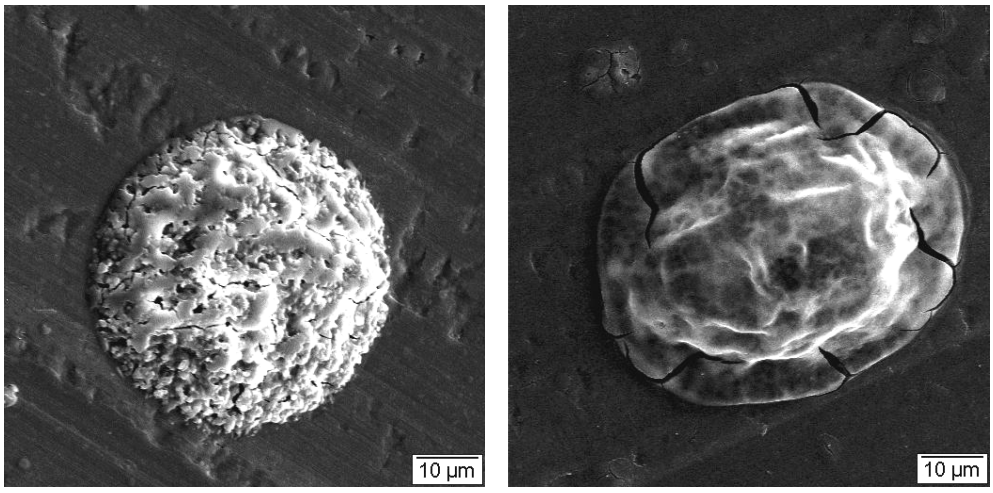

(a) (b)

Fig.23 Photographs showing a single droplet of (a) as-spun pure sol, and (b) pure sol calcined at 600^{o}C for 6 hr.

5.4.4 Jet evolution during electrospinning

The physical phenomena occurring during the electrospinning process were observed with a high speed digital camera. Quantitative results were observed under an electric potential of 30 kV. Sequential photographs illustrating the development of the jet and the breaking down of the jets

are shown in Figs. 24, 25 and 26. As shown in Fig. 24, polymer solution from the capillary forms the Taylor's cone and gradually breaks down from the capillary. The solution jet from the Taylor's cone is stretched by elongational flow. A continuous jet was then formed, followed by stable splitting or splaying. The electrospinning continues without many changes in the jet pattern. This observation is consistent with results reported by Tao [28]. In Fig. 25, during the electrospinning of pure sol, little elongational flow was observed due to the lack of solution viscosity. Jets blow out into droplets of various sizes because of the increased conductivity of the solution. The Taylor's cone pinched back after the initial spraying. New Taylor's cone would form after a short period of time. This time for the development of the new Taylor's cone was calculated to be 0.025s. Fig. 26 shows the electrospinning characteristics of the polymer/sol mixture. By combining the characteristics of both electrospun sol and polymer, some elongational flow was observed along with droplet formation. An unstable Taylor's cone may form before the bursting of the jet. This cone-shaped structure could pinch back and re-grow periodically. The average duration time for a single jet to break down is in the order of 0.066 s. This value is twice as much as the duration time of the pure sol. It has been reported by many investigators [35,55] that the addition of the sol significantly changes the electrical properties of the solution. Bulk conductivity was significantly increased and became the dominant factor to determine the morphologies of the jet during electrospinning. Thus, the jet is easy to be stretched and disintegrated to form droplets.

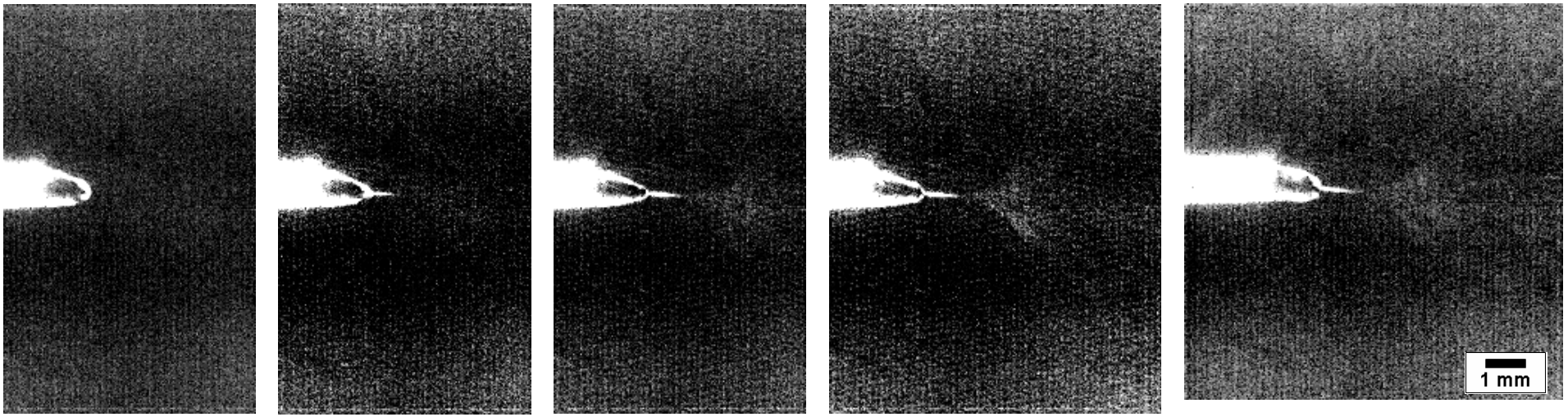

Fig.24 Sequential photographs showing the nature of the PVA aqueous solution jet for various times(s) after the application of the voltage. The voltage (30kV) was applied at t = 0 s.

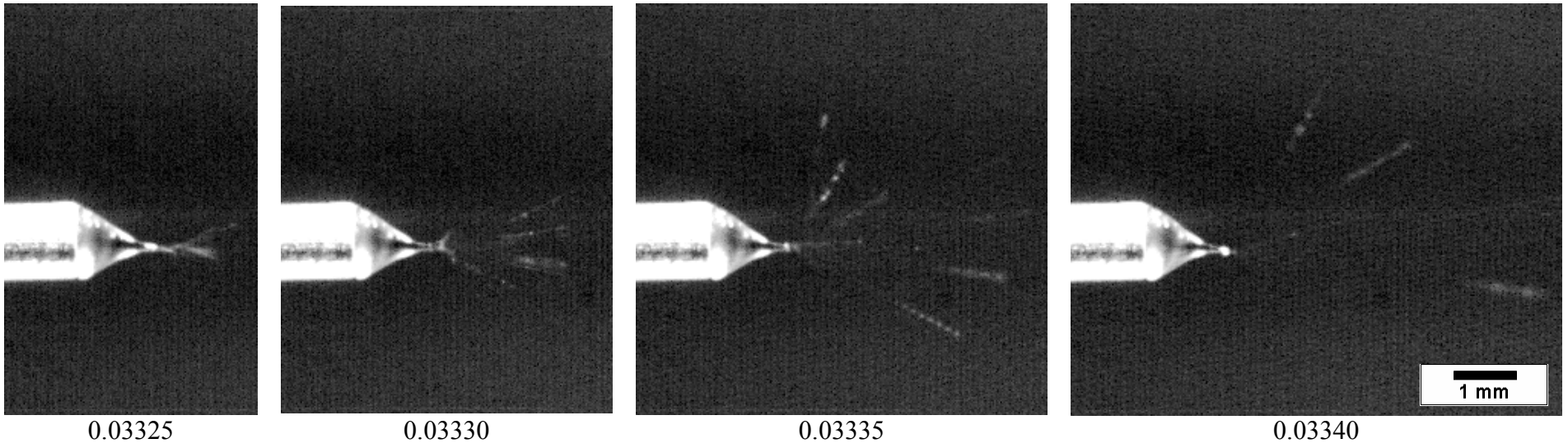

Fig.25 Sequential photographs showing the nature of the jet of pure sol for various times (s) after the application of the voltage (30kV).

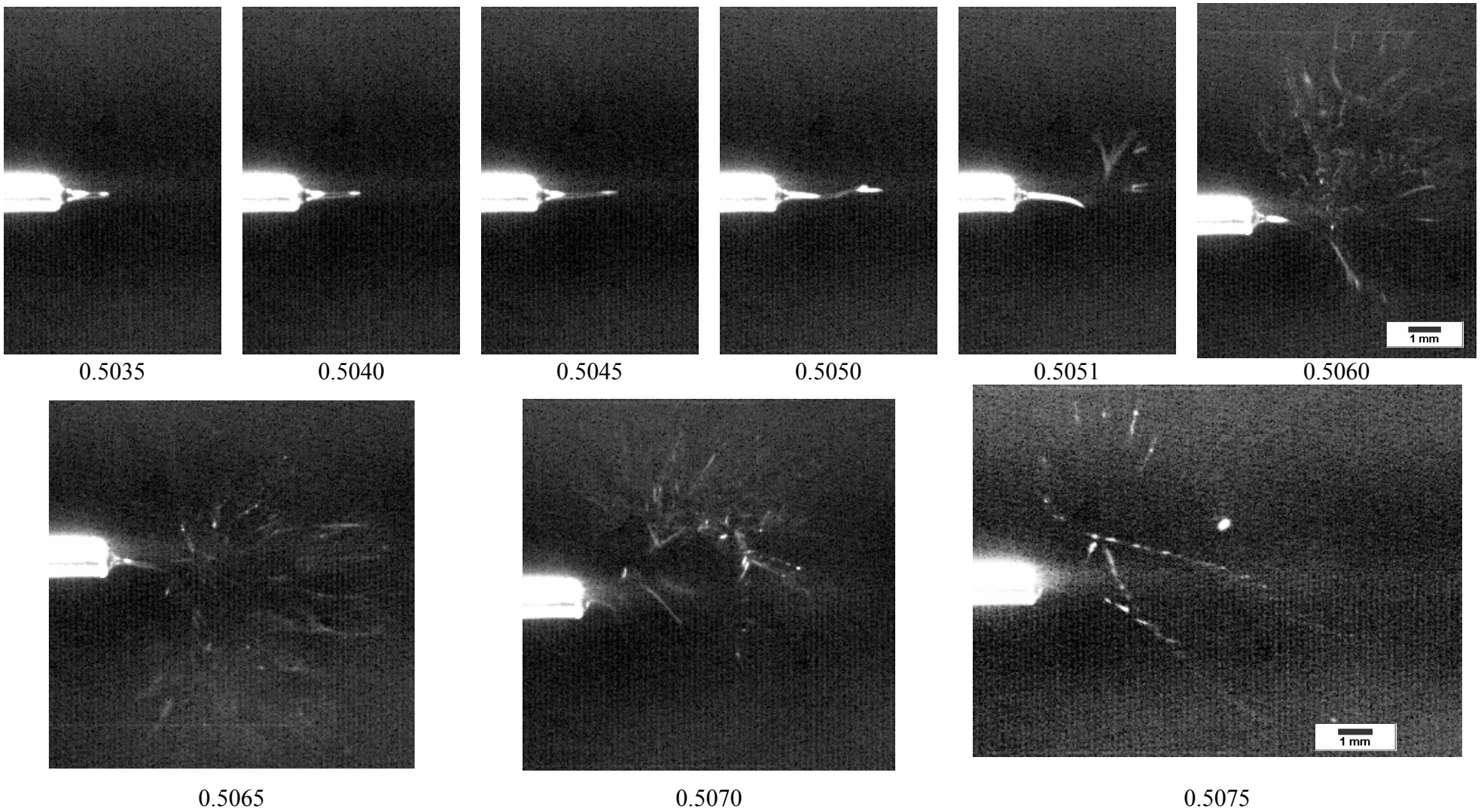

Fig.26 Sequential photographs showing the break down of the PVA/Sol solution jet after various times (s). The time is measured after the application of a voltage of 30kV.

5.4.5 Effect of M_W

It has been reported that formation of fiber after electrospinning relies on using polymer macromolecules to encapsulate the ceramic particles [35]. In order to achieve the continuous fibrous structures, the appropriate viscoelastic properties, such as viscosity and surface tension, of the polymer/sol mixture need to be established. In addition, two other conditions are required:

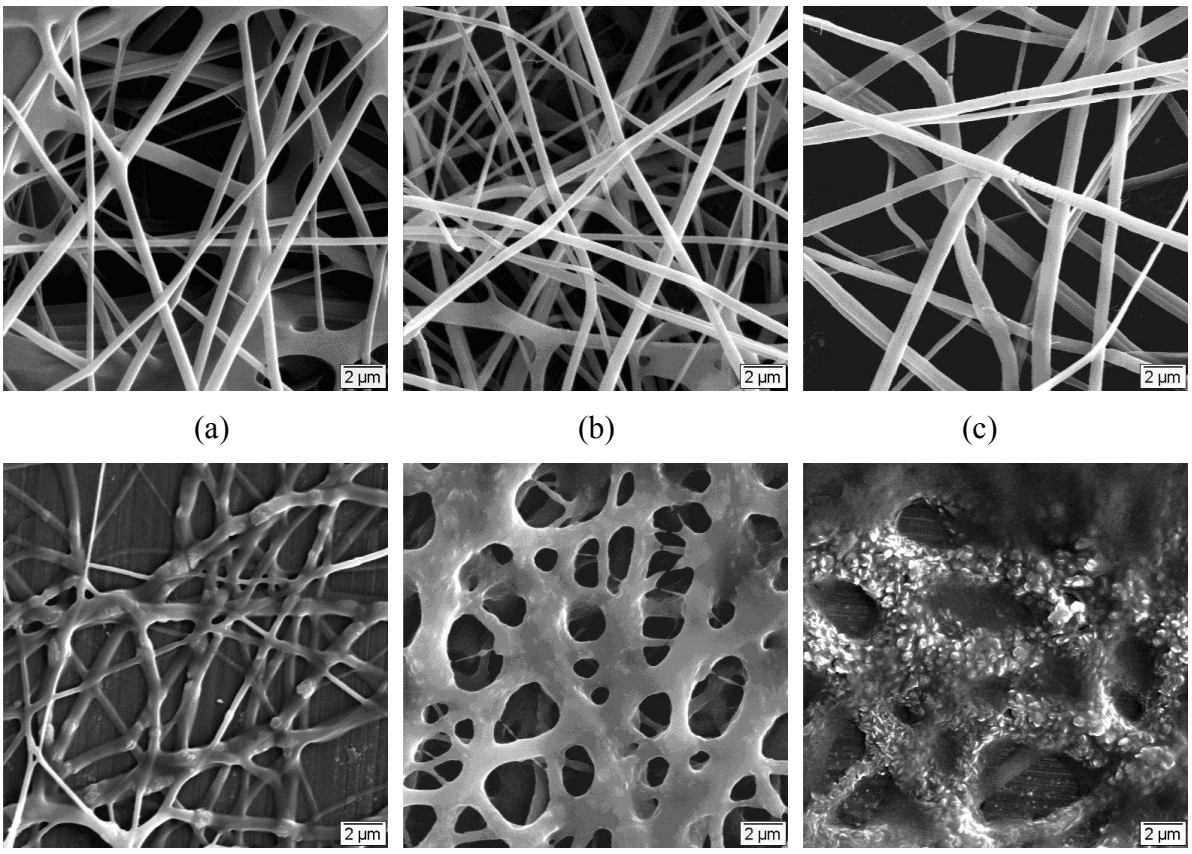

Fig.27 Photographs showing the as-spun structures for different volume fractions of the sol. (a) 0% (PVA aqueous solution); (b)16.7%; (c) 20%; (d) 25%; (e) 50%; (f) 66.7% (PVA M_W =155,000 g/mol).

1. A ceramic precursor with suitable particle size (*e.g.* < fiber diameter) and

2. A uniform dispersion of ceramic sol particles within the polymer matrix.

The small size of the sol particles can be achieved either through the chemical synthesis of the ceramic sol with submicron sized particles or by allowing the macromolecules to fully incorporate with the sol particles to decrease the theoretical size of the ceramic particles.

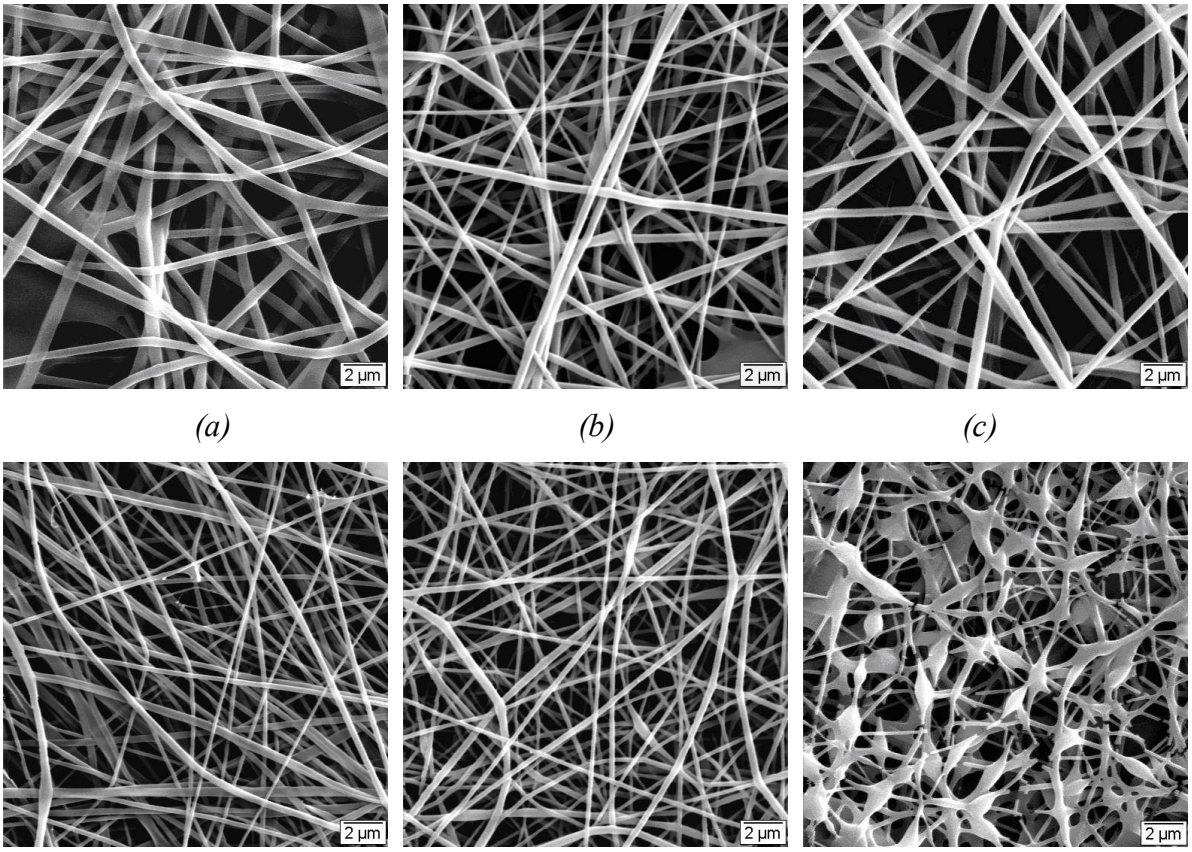

Fig.28 Photographs showing the as-spun structures for different sol volume fractions. (a) 0% (PVA aqueous solution); (b) 16.7%; (c) 20%; (d) 25%; (e) 50%; (f) 66.7% (PVA M_W = 67,500 g/mol).

In this work the second method was used for the dispersion of the sol. In this case, the water based sol and the hydrophilic polymer solution could provide good miscibility between the two phases. The issue of miscibility has not been studied in the literatures for electrospinning of ceramic fibers [35]. Adequate mixing time, which is also called, aging time, of the two precursors is critical to ensure proper miscibility. In the present work, a minimum aging time of 8 hr was used to achieve a good dispersion of polymer and sol phases.

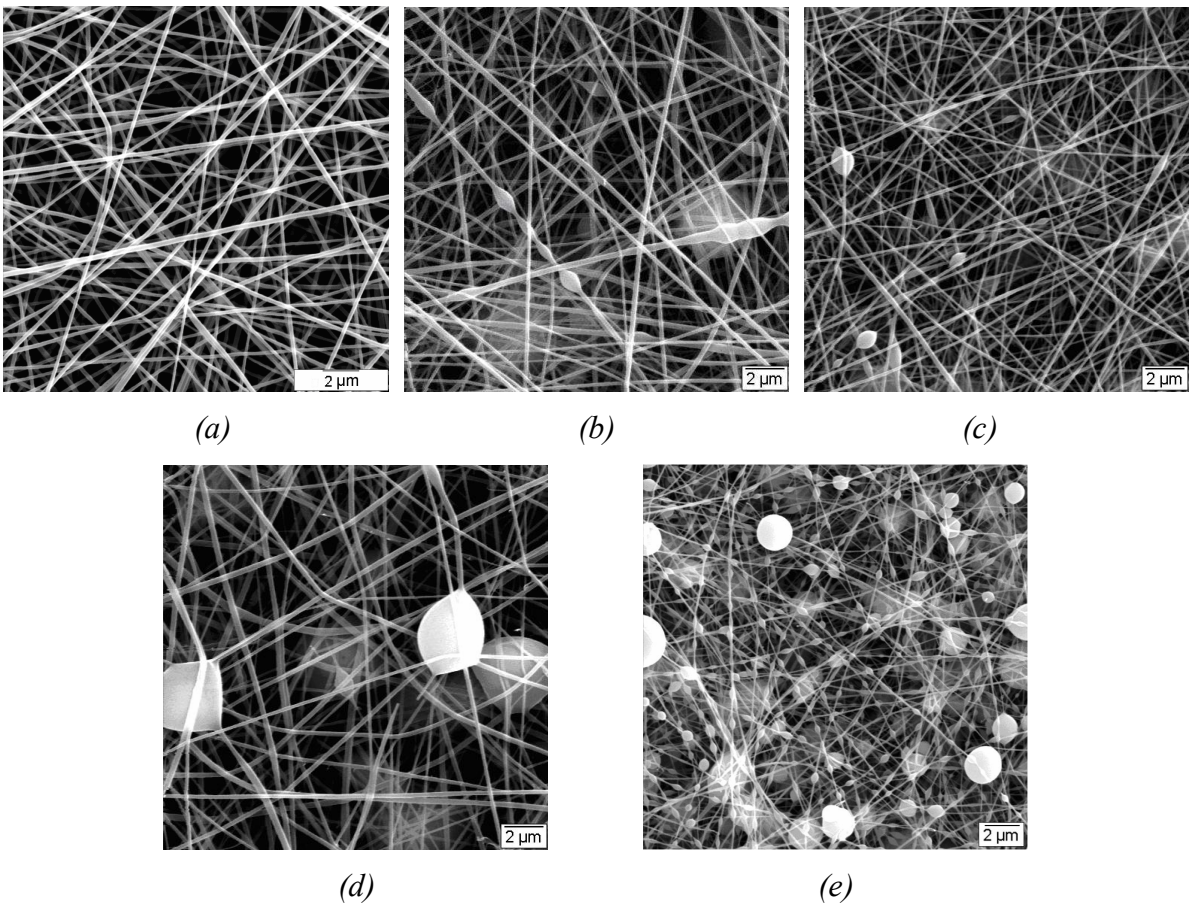

Fig. 29 Photographs showing the as-spun structures for different sol volume fractions. (a) 0% (PVA aqueous solution); (b)16.7%; (c) 25%; (d) 50%; (e) 66.7%. (PVA M_W = 40,500 g/mol).

The as-spun patterns of samples prepared by PVA (M_W = 155,000 g/mol) with different sol volume fractions are shown in Fig. 27. The sol particles started to be visible in the as-spun pattern for a sol volume fraction of 25%, which indicates the non-uniform mixing between polymer and sol. Even after mixing for 16 hr, sol particles can still be observed in the fibers. Thus, longer mixing time doesn't help achieving better mixing for this molecular weight.

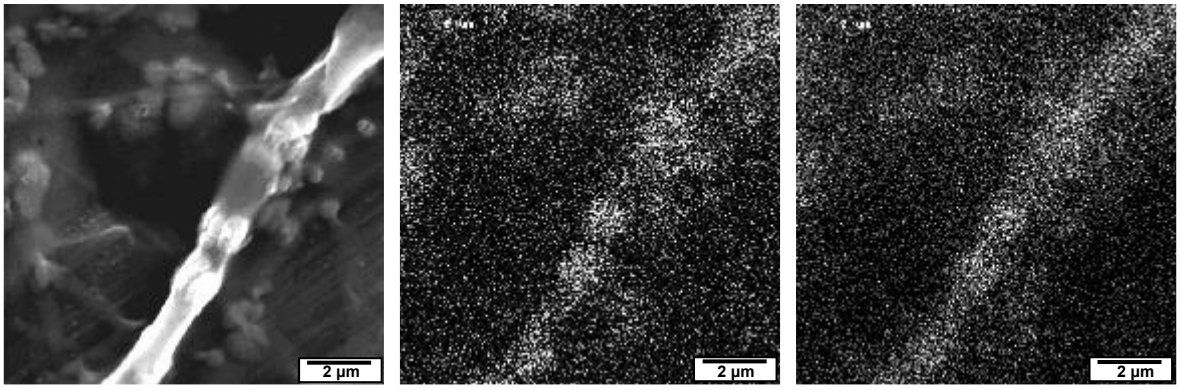

(a) *(b)* *(c)*

Fig. 30 Elemental map showing sol-particle-embedded fibrous structure. (a) SEM photograph, (b) phosphorus map, and (c) calcium map.

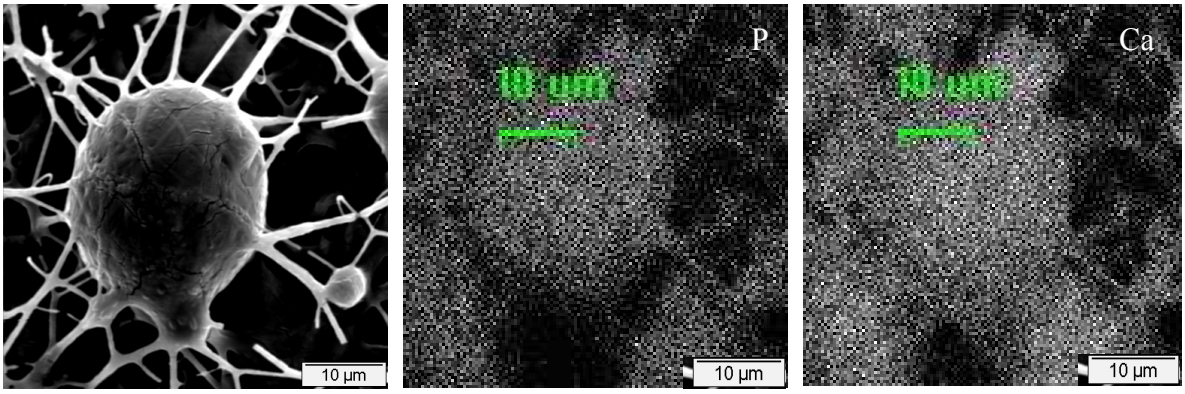

(a) *(b)* *(c)*

Fig.31 Elemental map showing droplets in the electrospun structure (a). The elemental maps for phosphorus (b) and calcium (c) are also shown.

Elemental mapping was conducted on these samples to examine the distribution of calcium and phosphorous. The highlighted regions in the elemental maps indicate the concentrated sol particles caused by the non-uniform distribution of the sol as shown in Fig. 30. Moreover, splats mainly composed of high amounts of sol were also observed in the sample as shown in Fig. 31.

Another series of experiments was carried out to verify the non-uniform distribution of the sol particles within the electrospun patterns. PVA/Sol mixture with PVA M_W = 155,000 g/mol and sol volume fractions of 20% and 25% were prepared and electrospun. Samples of the solution mixture were freeze dried before and after electrospinning. The solution mixture that was not electrospun was coated on a slice of glass before freeze drying. The SEM photographs are shown in Fig. 32.

A radiant structure with multiple leaflets of various sizes can be observed in all the samples. This structure may result from the agglomerated sol particles which tend to maximize the surface area for water loss during freeze drying. Large sized leaflet structures were observed in the sample without electrospinning (Fig. 32(a)). The SEM images of as-spun samples with sol volume fractions of 20% and 25% are shown in Figs. 32 (c) 32 (e), respectively. After freeze drying, the fiber diameters decreased due to the evaporation of the water content. In addition, different phases with varied concentrations are separated and are more noticeable in the pattern. For sol volume fraction of 20%, a limited number of the leaflet structures with a much smaller size were observed, as shown in Fig. 32 (b). These results suggest that during electrospinning the large sol particles can be broken apart into smaller particles along with the extensional

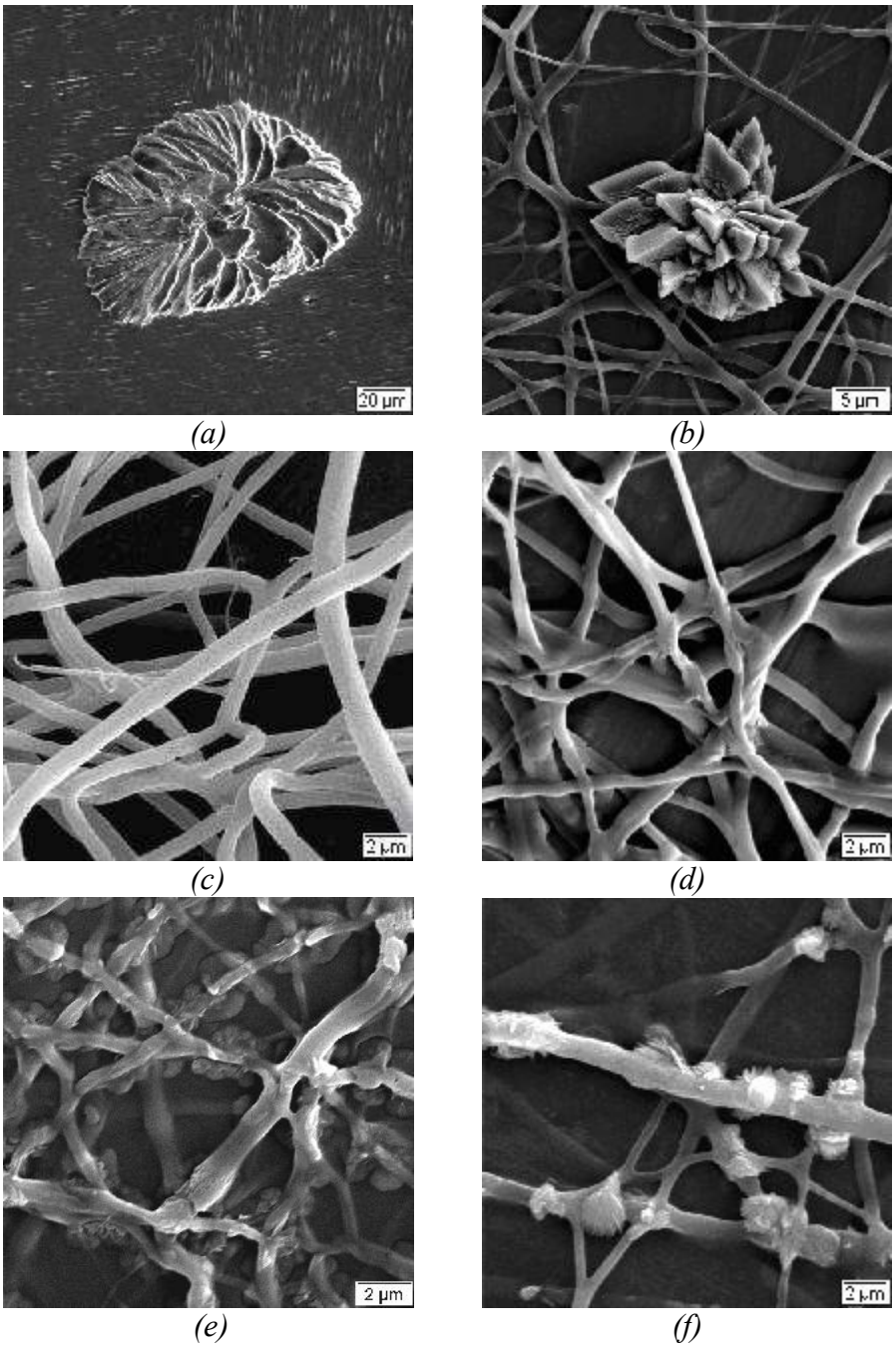

Fig.32 SEM photographs showing the structure in the polymer-sol mixture after various treatments (a) the original mixture (sol volume fraction of 20%) which was on a slice of glass and freeze dried. Photographs (c) and (e) are as-spun samples for sol volume fractions of 20% and 25%, respectively. Photographs (b) and (d) are the freeze dried as-spun samples for sol volume fraction of 20%. Photograph (f) is freeze dried as-spun sample of sol volume fraction of 25% (M_W=155,000 g/mol).

stretching of the polymer jet. Also, no evidence of embedded large sol particles was observed in the fibrous structure after freeze drying. However, sol particle with sizes smaller than the as-spun fiber diameter may be obtained.

The addition of inorganic phases to the polymer may result in the precipitation of these phases at high concentrations, as reported by Tao [28]. In their experiments, Tao [28] added NaCl particles to a PVA solution. Beyond a critical concentration of NaCl, a salting out phenomenon, where excess salt particles were observed in the structure, was reported. The data of Tao [28] show NaCl crystals throughout the sample beyond a critical concentration. This precipitation has been attributed to the reduced viscoelastic properties of the polymer solution upon the addition of the salt. Similar results were obtained in the present investigation as shown in Figs. 30 and 31. Thus, a sol volume fraction of 25% can be determined as the maximum concentration to

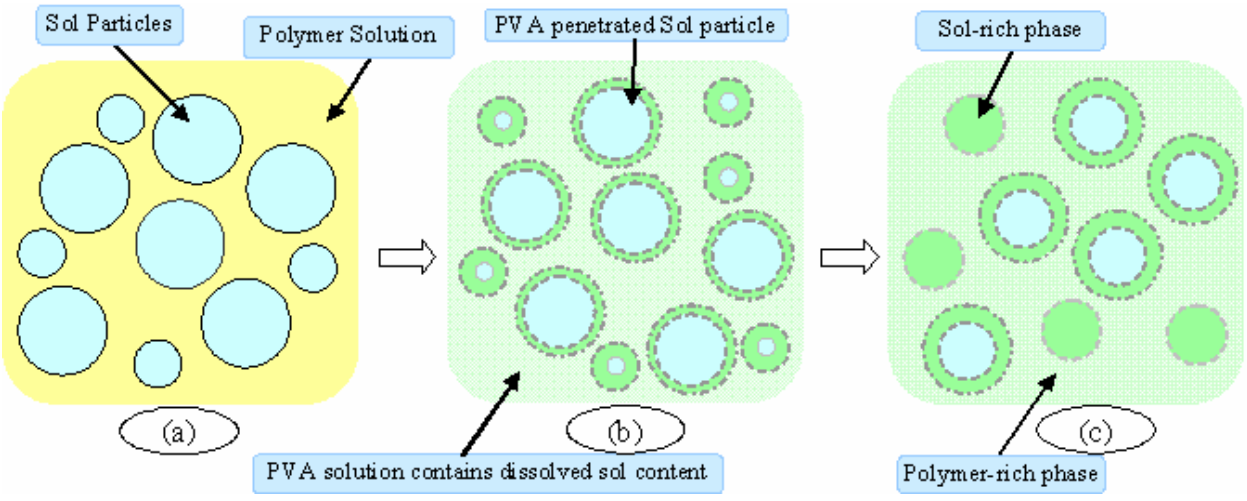

Fig. 33 Schematic illustrations showing the mixing of the polymer/sol mixture.

prevent the salting out phenomenon. Above this concentration, increasing amounts of sol particles can be observed in the as-spun sample as shown in Figs. 27 (e), and (f). The model shown in Fig. 33 may be used to explain these results.

As shown in Fig. 33 (a), two phases are present in the PVA/Sol mixture. Initially, the sol is dispersed within the polymer matrix in the form of various-sized particles. Upon mixing, two phases emerge over a period of time as shown in Figs. 33 (b) and (c). The polymer macromolecules can physically penetrate into the sol particles upon mixing. Some of the sol particles with this penetrated layer can then dissolve and be incorporated into the polymer solution upon mixing. The dispersion of the dissolved sol in the polymer matrix is originally not uniform. Hence, a polymer-rich phase (light green in Fig. 33) and a sol-rich phase (dark green in Fig. 33) may concurrently form in the mixture. Upon mixing, increasing amounts of sol can be dissolved and distributed in the polymer solution. The large sol particles within the mixture may be broken apart by vigorous stirring. Subsequently, when this solution is electrospun, three possible structures can be obtained: smooth fibers containing mostly polymer, thick fibers with embedded sol particles, and droplets containing large sol particles as shown in Fig. 34.

This model can well explain the formation of different morphologies obtained after electrospinning the PVA/Sol mixture prepared by PVA M_W = 155,000 g/mol and can also explain the morphology obtained after calcination.

The variation of fiber diameter upon adding the sol to the PVA solution with PVA Molecular weight of 155,000 g/mol is shown Fig. 35. The diameter initially decreases and then shows a

significant increase as the amount of sol is increased. The initial decrease in diameter may be attributed a reduction in the surface tension upon the addition of the inorganic phase. It has been reported that this reduction in surface tension may lead to fiber thinning, especially at high polymer molecular weights [28]. At higher sol volume fractions, the fibers formed may fuse

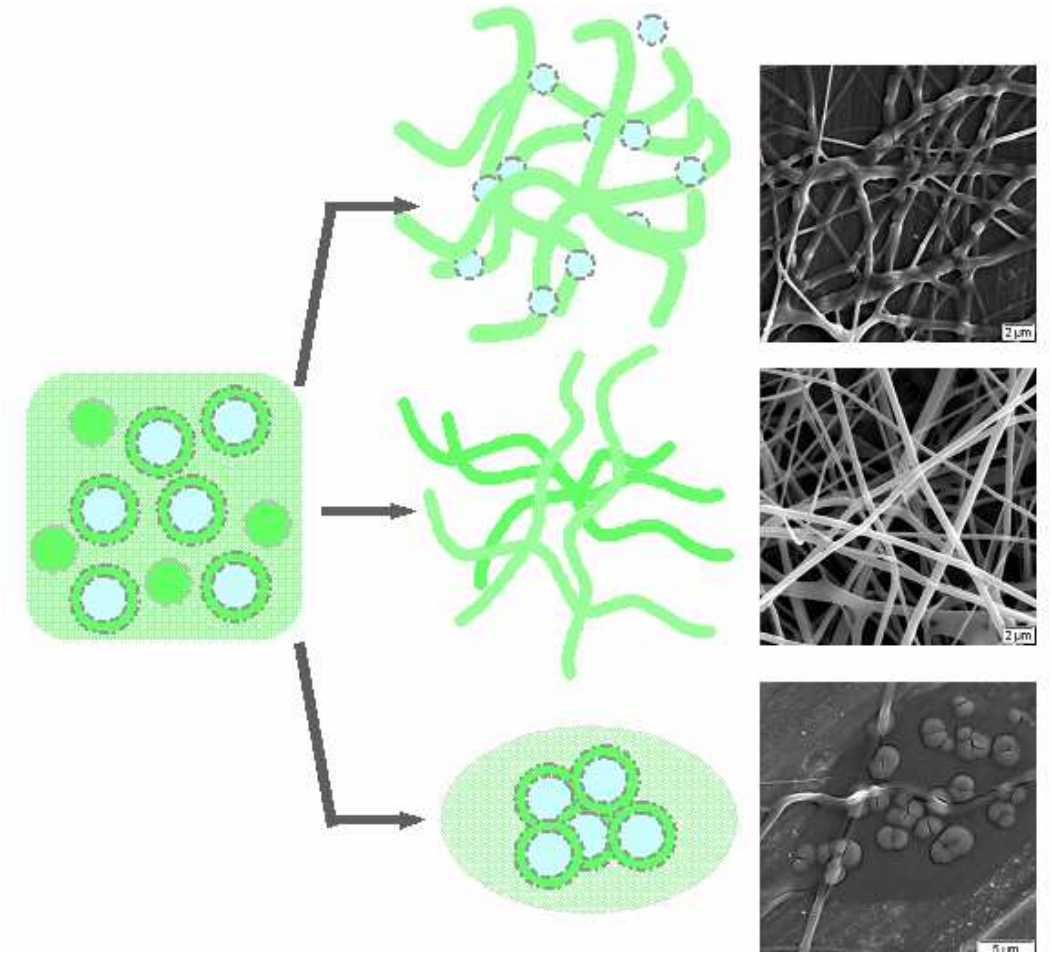

Fig. 34 Schematic illustration showing the development of various structures formed after electrospinning based on the model presented in Fig. 33.

together because of a lack of adequate solvent evaporation. Furthermore, the sol may also inhibit the splitting and splaying of the polymer fibers. Both these factors may lead to an increase in fiber diameter.

These results indicate that the lack of miscibility between the sol and a high M_W polymer might be the dominant factor that may determine the morphology of the as-spun pattern. This result is consistent with the results Viswanathamurthi *et al.* [41] who synthesized Niobium oxide fibers by mixing the Niobium oxide sol with PVAc aqueous solution. In their experiments, the fiber diameter of the higher loading samples (50vol% of sol) is twice as much as the diameter of the lower loading samples (20vol% of sol).

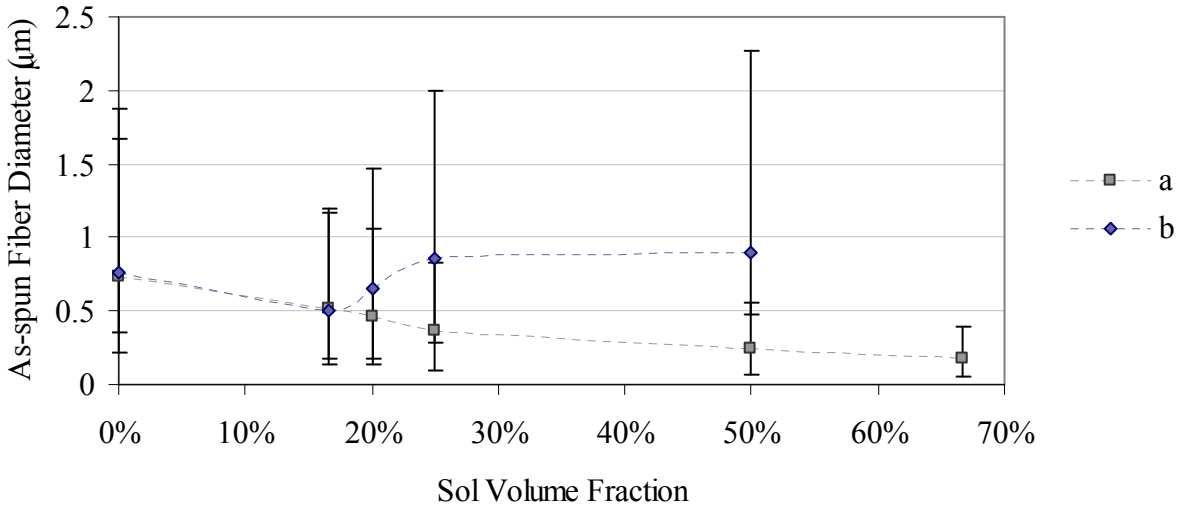

Fig. 35 Variation of the as-spun fiber diameter as a function of sol volume fraction. (a)PVA M_W of 67,500 g/mol, and (b) PVA M_W of 155,000 g/mol.

It has been reported that for the same *Berry* number, polymer solution with a lower polymer molecular weight may have lower viscosity. Furthermore, thinner fibers are obtained with lower

solution viscosity. The zero shear rate viscosities of PVA/sol mixtures for different PVA molecular weights are shown in Fig. 36. As can be expected, the zero-shear-rate viscosity decreases with increasing the sol volume fraction. As shown in Fig. 35, the fiber diameter decreases with increasing the sol volume fraction in the samples prepared by low molecular weight PVA. However, as the molecular weight of 155,000 g/mol, the fiber diameter increases with increasing sol. This result indicates that a reduction in solution viscosity may not be the dominant factor for determining the electrospun structure for high M_W samples. On the other hand, viscosity may play an important role in determining the electrospun structure of low molecular weight mixtures.

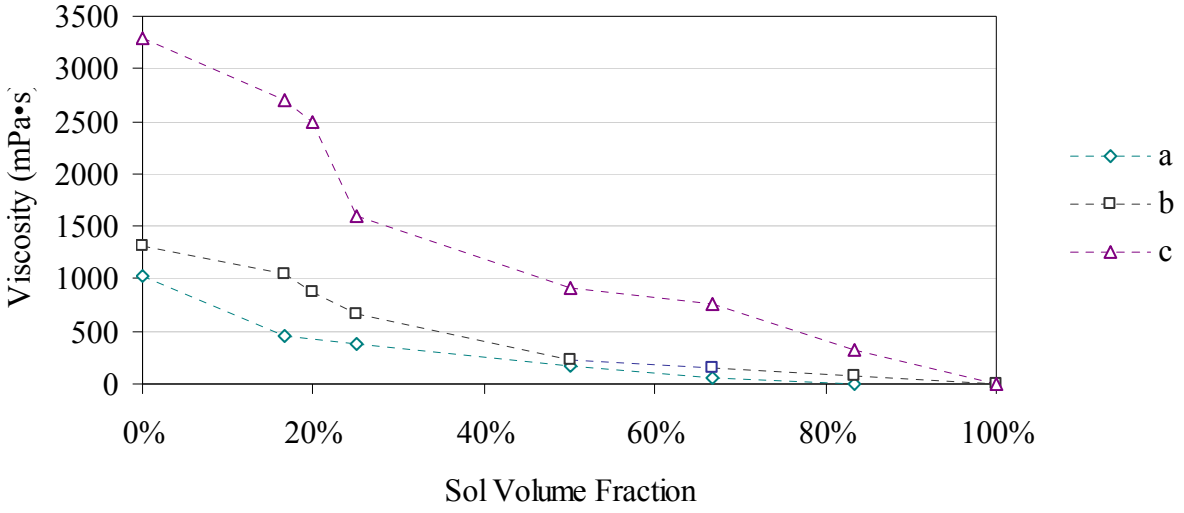

Fig. 36 Zero-shear viscosity as a function of sol volume fraction and molecular weight (a) M_W = 40,500 g/mol, (b) M_W = 67,500 g/mol and (c) M_W = 155,000 g/mol.

It is reported that a relatively low viscosity of polymer solution is necessary for uniform dispersion of the sol particles within the polymer matrix [27]. Hence, it is easier for a low M_W polymer solution to achieve better mixing between the PVA solution and the sol. A

homogeneous solution will be obtained after mixing. In these systems, the viscoelastic property may have the greatest effect on electrospun fiber morphology. While, in the non-uniform systems, such as the high molecular weight mixtures, the splitting of the jets during electrospinning was disrupted by the sol particles present within the polymer matrix. Thus, the effects of viscosity may be minimized.

5.4.6 Calcination

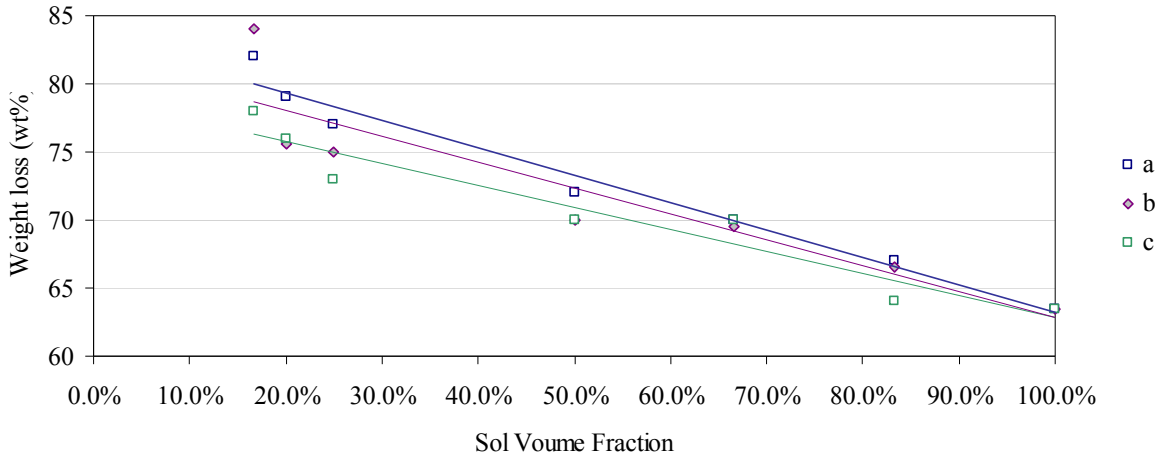

Fig. 37 Weight loss after calcination of the electrospun polymer as a function of sol volume fraction. (a) M_W = 40,500 g/mol, (b) M_W =67,500 g/mol, and (c) M_W = 155,000 g/mol.

The weight loss upon calcination as a function of polymer molecular weight is shown in Fig. 37. The weight loss in the high M_W sample was slightly lower than the in the low M_W samples because of the lower polymer concentration. The total weight decreases almost linearly with increasing sol content, suggesting that polymer can be totally eliminated upon calcination. Upon calcination, different fibrous structures were obtained. Figs. 38 - 41 show the different morphologies obtained after calcination.

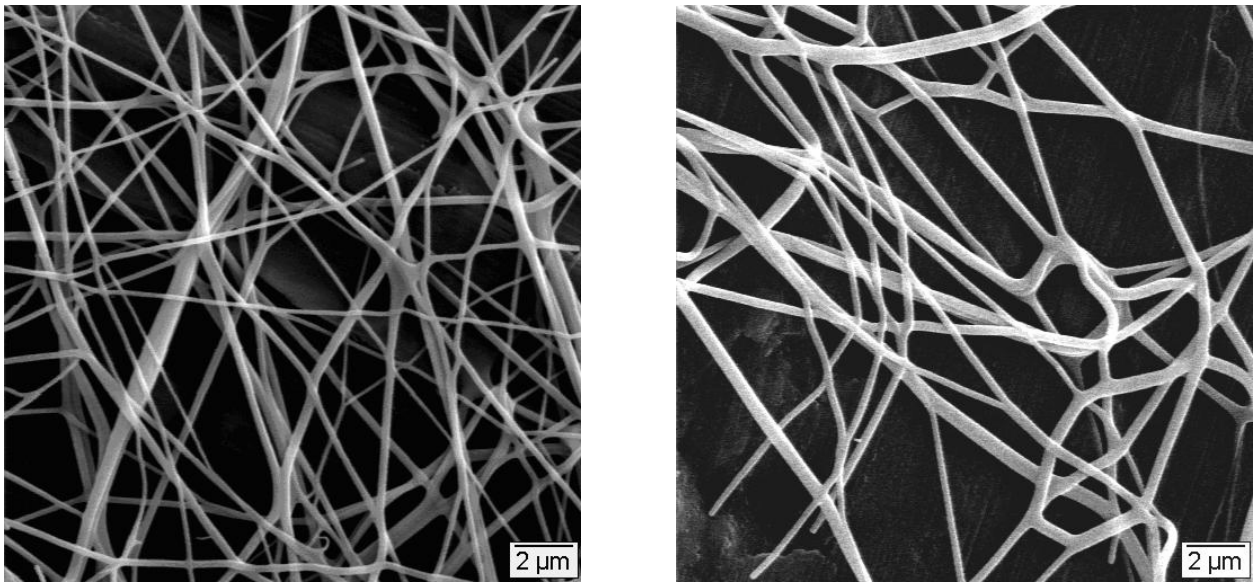

(a) *(b)*

Fig.38 Photographs showing solid fibers after calcination with (a) Sol volume fraction = 16.7%, and (b) Sol volume fraction = 20% (PVA M_W = 155,000 g/mol).

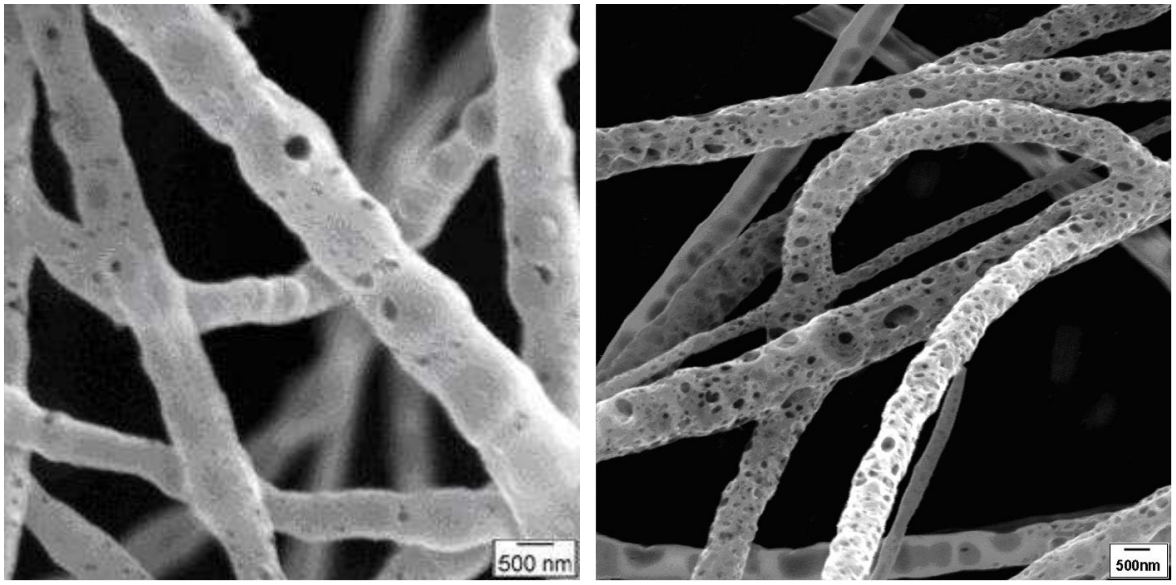

(a) *(b)*

Fig. 39 Photographs showing porous fibers with (a) Sol volume fraction = 16.7% and (b) Sol volume fraction = 20% (PVA M_W = 155,000 g/ mol).

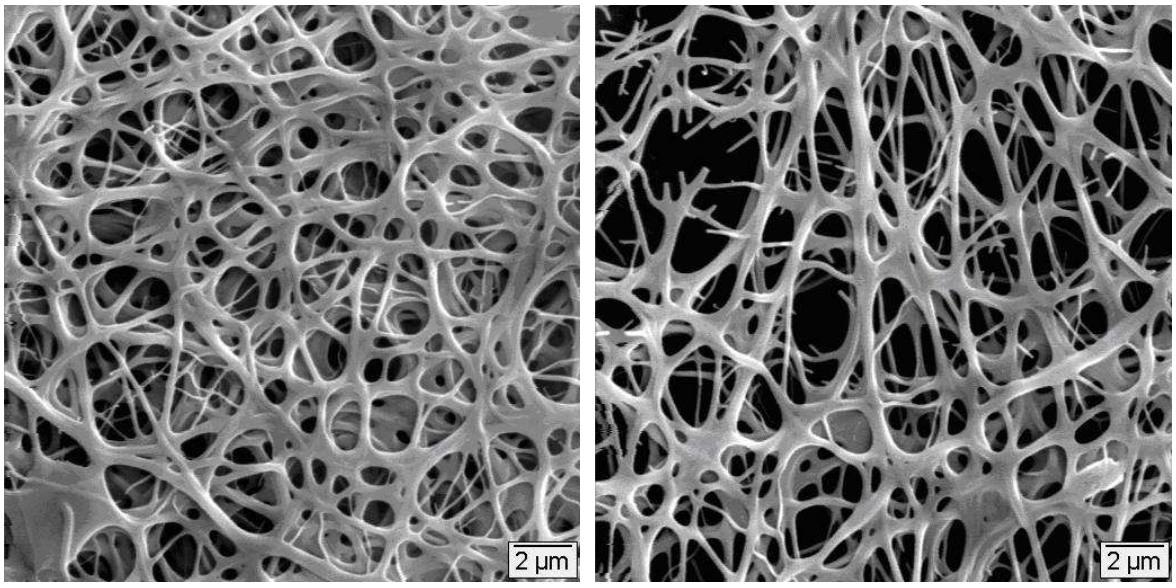

(a) *(b)*

Fig. 40 Photographs showing highly interconnected structures after calcining at 600°C for 6 hr for sol volume fractions of (a) 16.7% and (b) 20% (PVA M_W =67,500 g/mol).

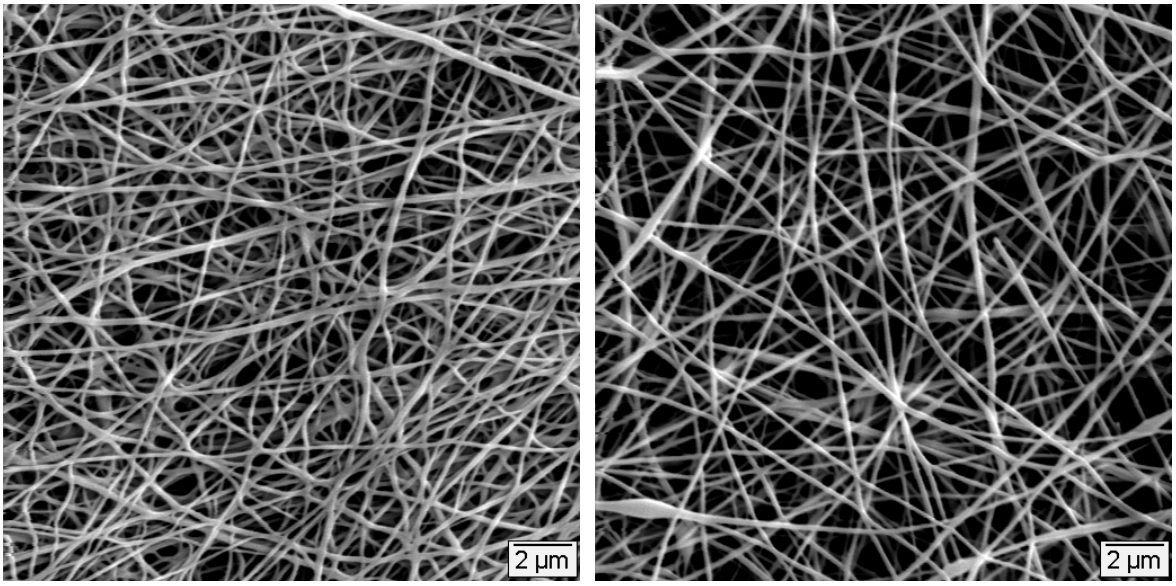

(a) *(b)*

Fig. 41 Photographs showing fibrous structures after calcining at 600°C for 6 hr for sol volume fractions of (a) 25% and (b) 50% (PVA M_W = 67,500 g/mol).

The as-spun fibrous morphologies were generally retained after calcination. Fibers and some beads with much smaller diameters than in the as-spun structures were obtained. Upon calcination of the dried sample, a consolidation reaction occurs. The sol particles tend to sinter together to minimize the surface area. The ratio between the diameters of the calcined and as-spun fibers is shown in Figs. 42. It can be seen from Fig. 42 that the average fiber diameter for M_W = 67,500 g/mol increased slightly after calcination. This is because of the fibers with small diameters were stretched out during the consolidation reaction and broken apart by the heat flow during calcination. The average fiber diameters after calcination for the condition of sol volume fraction of 25% and 50% are 170 nm and 190 nm, respectively. The effects of the consolidation reaction will be discussed in detailed in the following section.

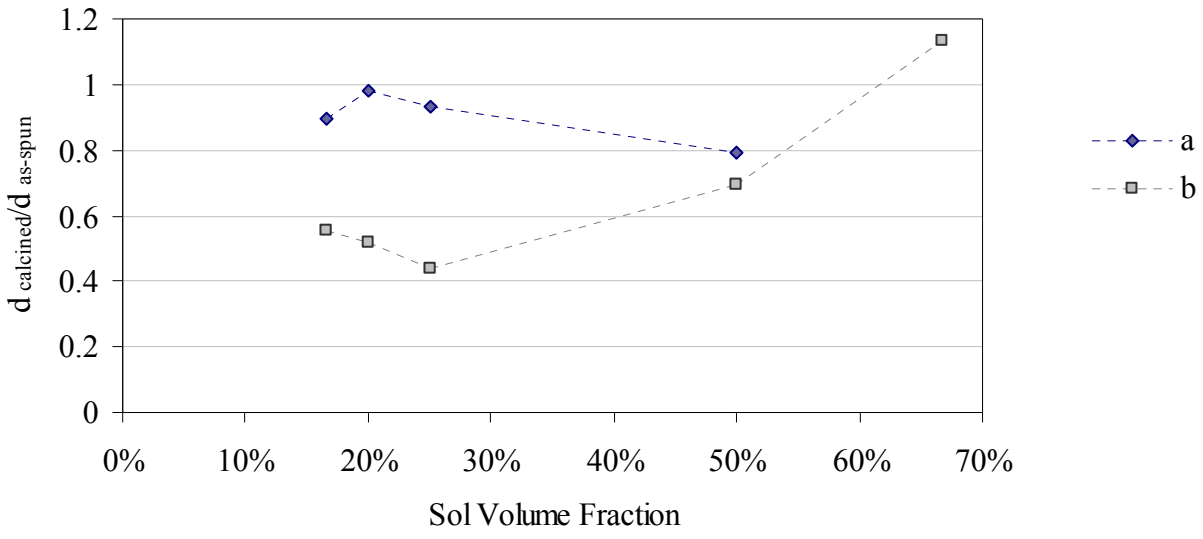

Fig. 42 Variation of the fiber diameter before ($d_{as\text{-}spun}$) and after ($d_{calcined}$) calcination as a function of sol volume fraction (a) M_W =155,000 g/mol, and (b) M_W =67,500 g/mol.

Based on the results presented above, the final structures after calcination have been categorized into single fibers, interconnected scaffolds and beads/beads-on-fibers structures. The possible mechanisms that result in each of these structures are discussed in the following sections. Two basic morphologies of single fibers were observed, solid fibers (Fig. 38) and porous fibers (Fig. 39). Porous fibers were generally detected in samples produced with sol volume fraction of 20% and 16.7%. A mixture of porous and dense fibers, with porous fibers porous fibers being the smaller fraction were observed in many samples. The two morphologies often occurred

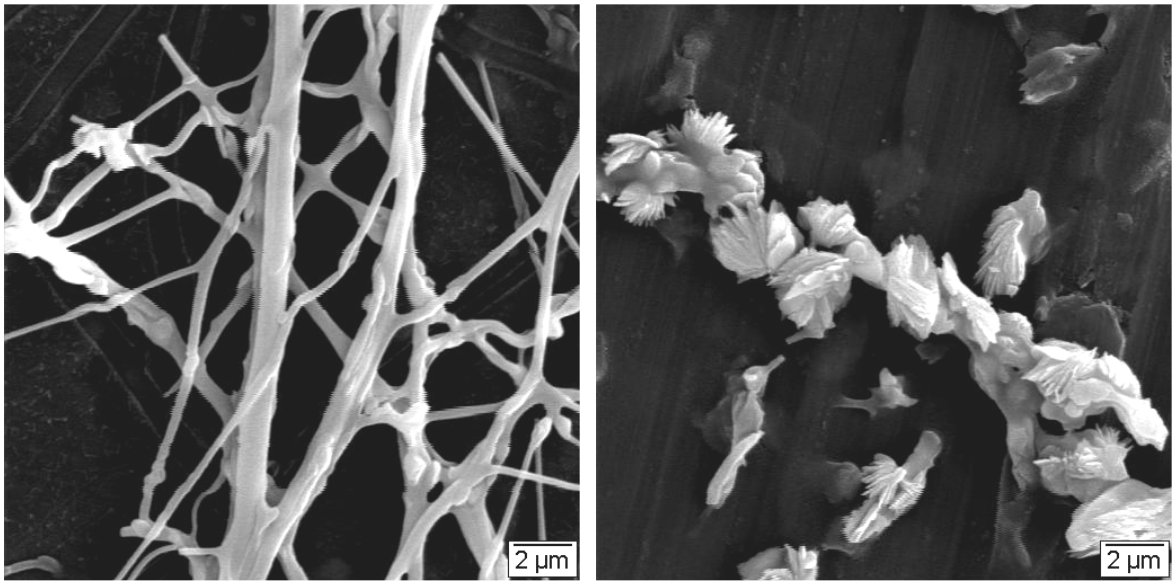

(a) *(b)*

Fig. 43 Photographs showing freeze dried samples after calcination at 600^{o}C for 6hr. (a) Sol volume fraction = 20%, and (b) Sol volume fraction = 25% (PVA M_W = 155,000 g/mol).

randomly in the calcined samples. It is likely that different fibrous morphologies may originate from the different phases that may be present in the polymer/sol mixture as discussed in Fig. 33. The solid single fibers may originate from the polymer-rich phase in the mixture, while the

porous single fibers may form from the sol-rich phase. During sintering, the fibers from the polymer-rich phase tend to form a smooth surface due to the smaller size of the sol particles dispersed within the polymer phase. The fibers from the sol rich phase contain larger particles. The polymer may occupy the space between these particles. During calcination, the sol particles may be sintered together, while the polymer content may be burnt out. Thus, fibers with pores may be obtained. As shown in Fig. 39, the pore size and the amount of pores in the calcined sample with sol volume fraction of 16.7% are generally smaller than in samples with a sol volume fraction of 20%. This difference further proves that better mixing is achieved by lowering the sol content.

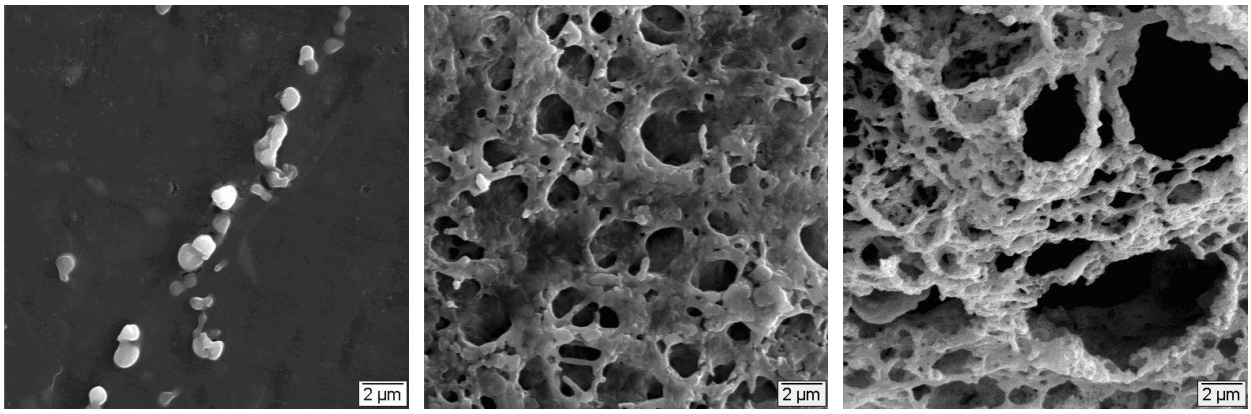

(a) *(b)* *(c)*

Fig. 44 SEM photographs showing the calcined structures of (a) Sol volume fraction = 25% (b) Sol volume fraction = 50% (c) Sol volume fraction = 83.3% (PVA M_W= 155,000 g/mol).

The SEM images of the freeze dried samples that have been calcined are shown in Fig. 43. Small particles within fibers are more visible in the calcined freeze dried sample of sol volume fraction of 20% (Fig. 43 (a)) compared to the freeze dried as-spun sample (Fig. 32 (d)). It should

be noticed that the sol particles with size smaller than the fiber diameter emerged after calcination in the freeze dried samples (Fig. 43(a)). The radiant structure indicating the non-uniform mixing of the sol and polymer can further be clearly observed at higher sol contents (Fig. 43 (b)). The calcined structures for sol volume fraction of 25%, 50% and 83.3% are shown in Fig. 44. The morphology of sol particle is more pronounced in these samples.

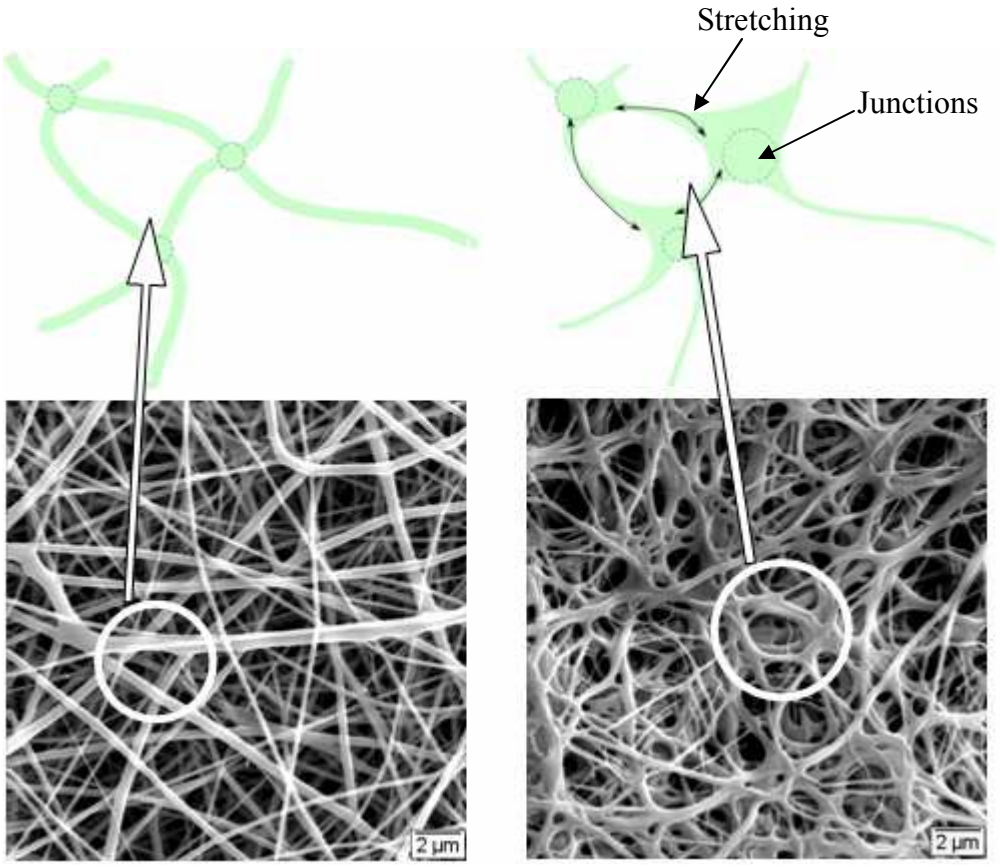

(a) *(b)*

Fig. 45 SEM photographs are shown before (a) and after (b) calcining. The highlighted regions are shown in detail to outline the formation of interconnected porous structures for the two cases. The stretching of the fibers between junctions are illustrated (PVA M_W = 67,500 g/mol).

Highly interconnected structures formed after calcining the samples of sol volume fraction of 16.7% and 20% by using PVA with M_W = 67,500 g/mol (Fig. 40). The formation of these highly interconnected structures can be explained as follows (Fig. 45). A fiber mat with a high fiber density forms after electrospinning the polymer-sol mixture. As a result, there are a large number of intersections between fibers, at which sol particles may sinter together and form junctions. The remaining sol particles may be stretched towards the ends and connected at the junctions (Fig. 45). Note that a more open structure with thinner fibers between the junctions is obtained with sol volume fraction of 20% than a fraction of 16.7% because of the initial electrospun structure. As discussed before, the thinner fibers are obtained upon electrospinning as the sol content increases from 16.7% to 20%.

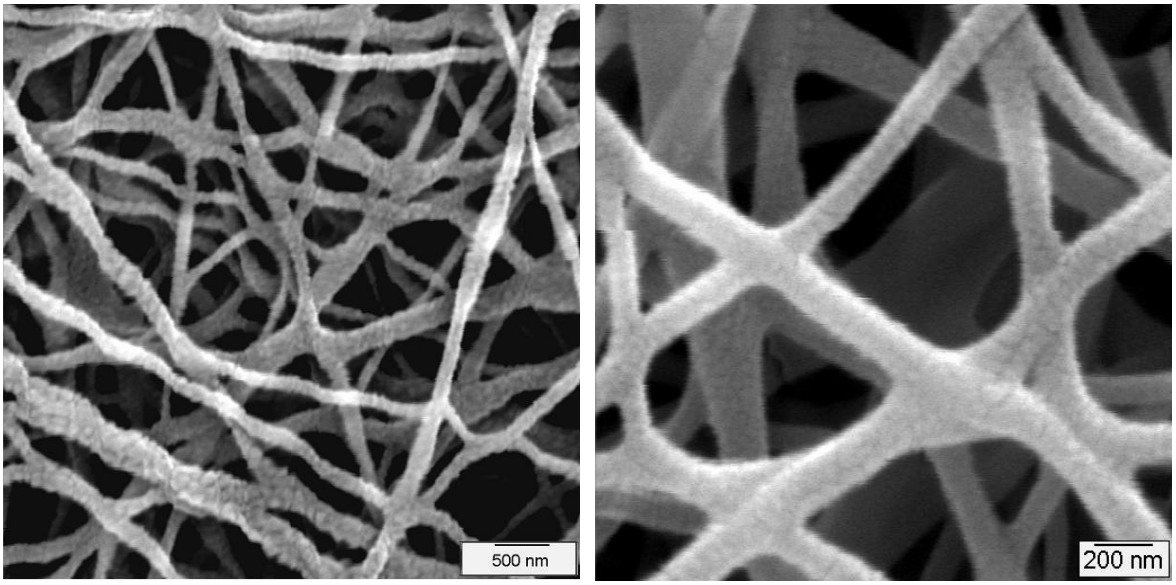

(a) *(b)*

Fig. 46 High Magnification photographs showing the calcined samples with sol volume fractions of (a) 25% and (b) 50% (PVA M_W = 67,500 g/mol). Notice the average fiber diameter is 170 nm and 190 nm, respectively.

Fibers with fiber diameter as low as 170nm can be obtained for sol volume fractions of 25% and 50% with PVA M_W =67,500 g/mol as shown in Figs 41 and 46. These conditions can then be considered as the optimum conditions to obtain ultra fine interconnected fibers. As the molecular weight is reduced further to 40,500 g/mol, no fibrous structures were obtained after calcination as shown in Fig. 47. In this case, the very thin fibers produced upon electrospinning appear to break apart during calcination. The broken fragments can then agglomerate together to form a dense mass as shown in Fig. 47 (b).

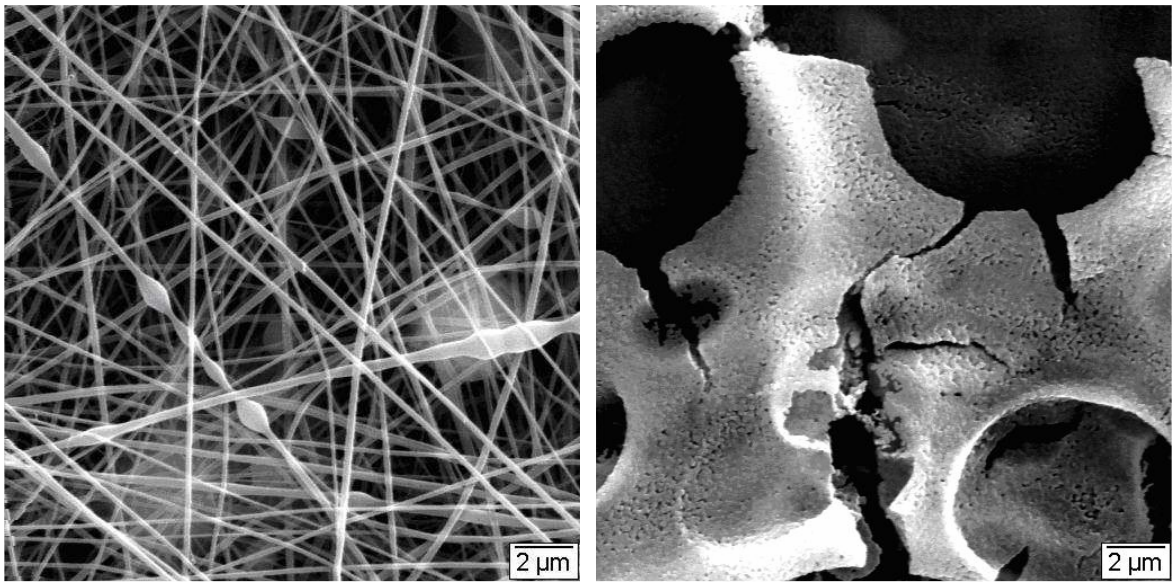

(a) *(b)*

Fig. 47 Fibrous structure with high fibrous density is amalgamated to form a flat pattern. PVA M_W=40,500 g/mol, sol volume fraction = 16.7%.

When a bead-on-string structure is obtained during electrospinning, the fibers between beads can be stretched out significantly during calcination (Fig. 48). Some of these stretched fibers can break apart. It appears that the ratio between the bead diameter and the fiber diameter plays a

critical role in the preservation of the fibrous structure. As the ratio between the bead diameter and the fiber diameter in the original sample becomes large, the bead on string structure can also be retained in the calcined sample as shown in Fig. 49. Fibrous structure can still be observed in these samples. The ratio between the fiber diameter and bead diameter for sol volume fraction of 25%, 50% and 83.3% are measured from the as-spun structures shown in Figs. 29 (c), (d) and (e) to be 4, 5.5 and 6.5 respectively. Some thick fibers can still be retained even in the presence of large beads with bead to fiber ratios as high as 6.5.

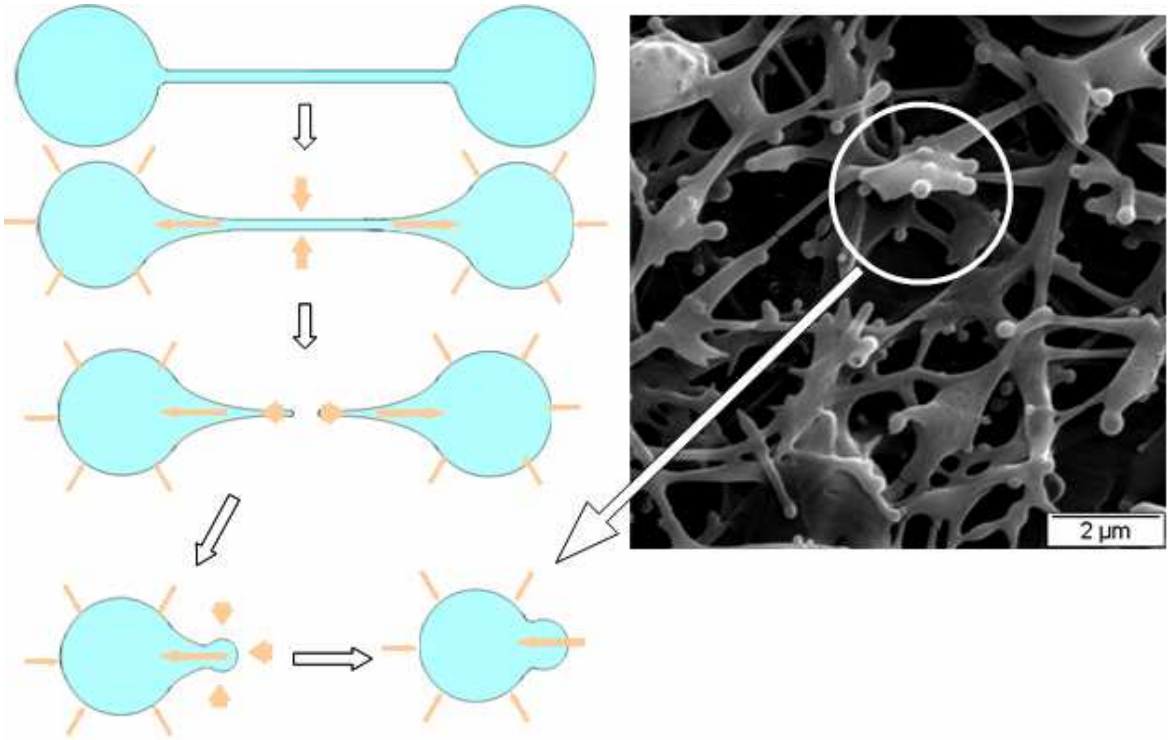

Fig. 48 Schematic illustration of the effects of calcination in bead-on-string structure obtained after electrospinning. The stretching of the fiber between the beads is demonstrated. The SEM photograph shows the structure in the calcined sample and the inset shows the bead after calcination. (Sol volume fraction = 83.3% and PVA M_W = 67,500 g/mol).

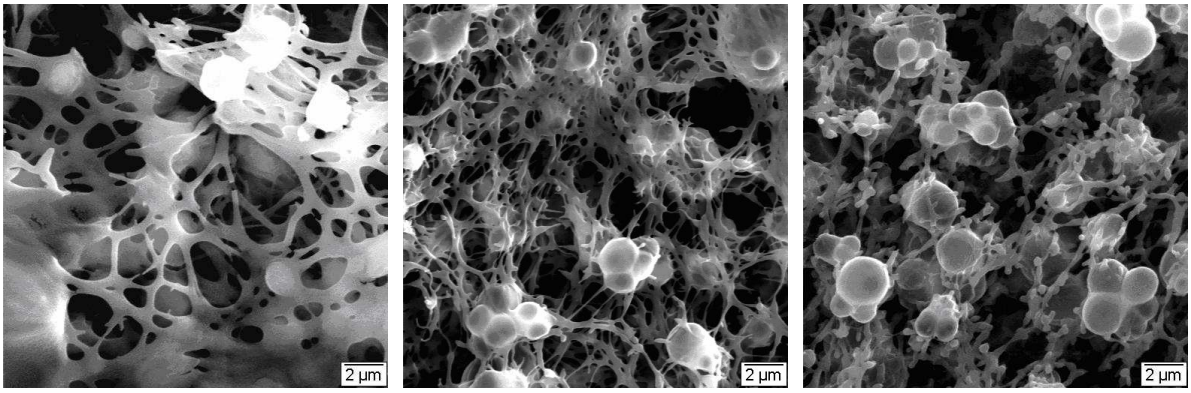

(a) (b) (c)

Fig. 49 Photographs showing bead-on-fiber structure obtained after calcination for different sol volume fractions. The structure before calcination is shown in Figs. 29 (c), (d) and (e). The volume fractions of the sol are (a) 25%, (b) 50%, and (c) 66.7%. (PVA M_W = 40,500 g/mol).

As the bead to fiber ratio in the electrospun mixture increases even further, at some critical point only beads may be retained after calcination. Hence, even though fibers may be present in the electrospun structure, upon calcination the sample may consist only of beads. In order to verify this hypothesis, experiments were conducted under conditions where a bead-on-string structure with large beads would result after electrospinning. Experiments were conducted at Be = 9 to fulfill this requirement. The data shown in Fig. 50 indeed indicate that as the ratio between the bead diameter and fiber diameter is increased above 9, only beads remain after calcination. It also appears that the beads are sintering together during calcination.

The effect of sol volume fraction on the XRD pattern is shown in Fig. 51. It can be seen that this fraction did not have significant effect on the crystal structure. Crystal sizes were measured to be on the order of 10-15 nm. This value is much smaller than the value obtained with powders produced from pure sol (30 nm). Thus it appears that electrospinning does seem to reduce the

crystal size in the ceramic. Several investigators have reported that the crystal size in the polymer decreases upon electrospinning [60]. A similar effect may be observed in the calcined ceramic. The molecular weight of the polymer did not have a significant effect on the crystal size. It appears that the crystal size is primarily determined by the fiber diameter. The crystal size generally decreases with the diameter of the fiber produced after electrospinning.

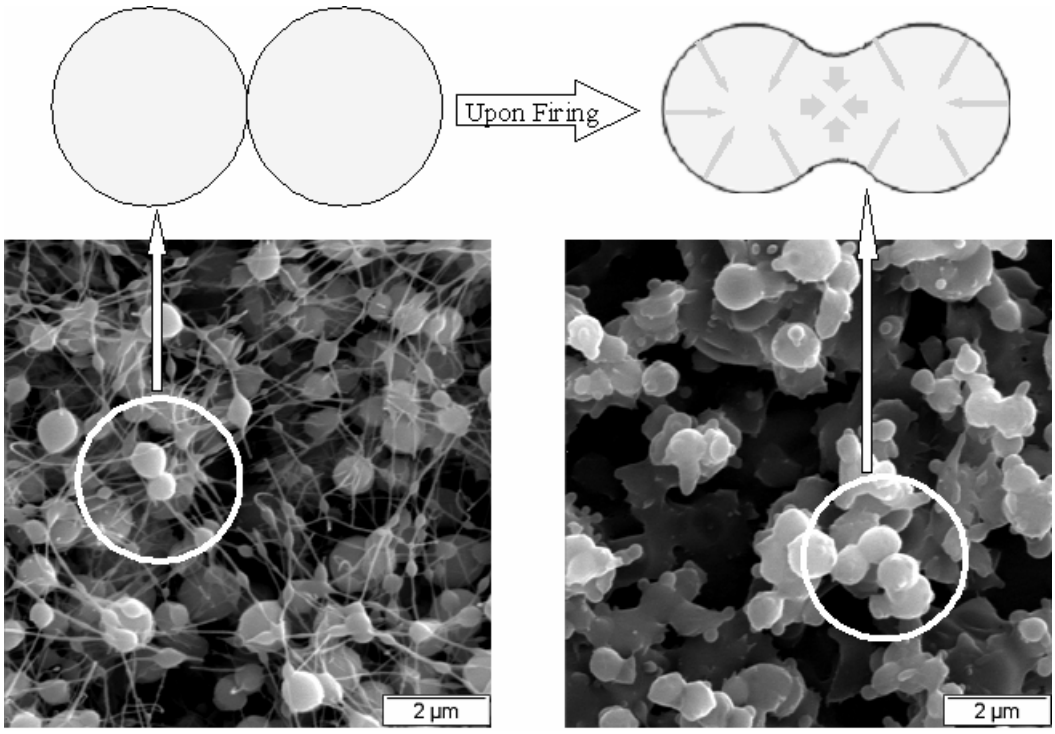

(a) *(b)*

Fig. 50 *Photographs showing the bead-on-string structure after electrospinning (a). The corresponding structure after calcination is shown in (b). The inset highlights the sintering of beads upon calcination. (PVA M_W = 40,500 g/mol, the Be number of the polymer solution is 9, sol volume fraction of 66.7%).*

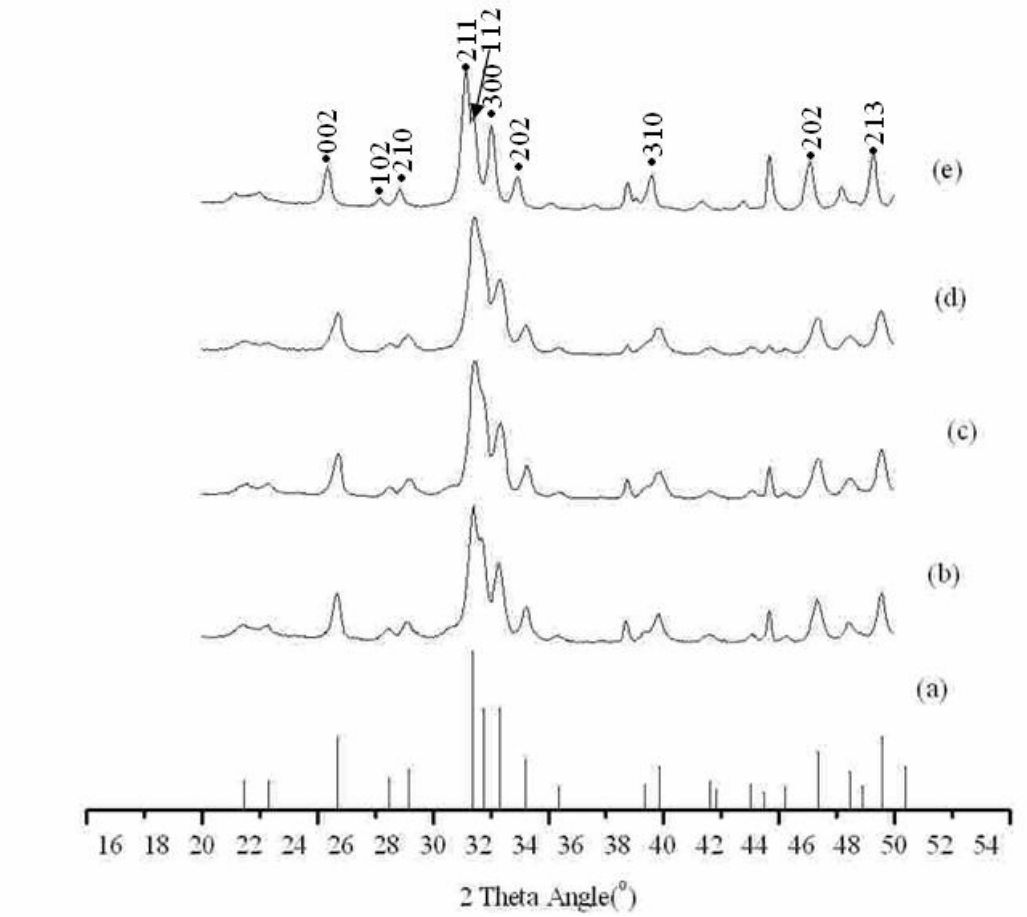

Fig. 51 XRD pattern for samples calcined at 600°C for 6 hr. (b) Sol volume fraction = 16.7%, (c) Sol volume fraction = 20%, (d) Sol volume fraction = 25%, and (e) Sol volume fraction = 50%. The JCPDS file (#09-0432) for hydroxyapatite is also shown in the bottom of the figure (a). The peaks for hydroxyapatite (●) are indicated.

5.5 Conclusions

Calcium phosphate fibrous networks were produced after calcination of an electrospun PVA/sol mixture. The polymer molecular weight and the sol volume fraction have significant effect on the electrospun pattern. At high M_W (155,000 g/mol), the mixing conditions have significant effects on the electrospun structures. As the volume fraction of the sol is increased to 25%, a

large number of sol particles may be present in the fibers. As a result, a thicker fibrous structure is obtained. As the M_W is decreased to 67,500 g/mol, the solution viscosity has a major influence on the as-spun structures. In this case, a stable fibrous structure with a uniform dispersion of sol particles was obtained. As the M_W of the polymer is further reduced to 40,500 g/mol, a bead-on-string structure was obtained after electrospinning. In this case, a mixture of beads and fibers was obtained after calcination. A polymer/sol mixture with PVA molecular weight of 67,500 g/mol and sol volume fraction between 20% and 25% were most effective in producing an interconnected fibrous network after calcination. Fibers with diameter as low as 170 nm were obtained under these conditions. A continuous fibrous network could be obtained for molecular weights of 155,000 g/mol and 67,500 g/mol. In general, uniformly distributed structures can be obtained by increasing the sol volume fraction or decreasing the polymer concentration. XRD analysis indicated hydroxyapatite to be the dominant inorganic phase remaining after calcination with crystal sizes on the order of 10 to 30 nm.

6. CONCLUSIONS

Calcium phosphate fibrous networks with average fiber diameter between 200 nm to 2 μm were produced after calcination of an electrospun PVA/calcium phosphate based sol precursor. After calcination, the polymer phase can be removed and the fibrous structure can be retained in the inorganic phase. The M_W of the polymer had a significant effect on the final structure obtained after calcination. Complete fibrous structures were obtained after electrospinning and calcination for M_W = 155,000 g/mol and M_W = 67,500 g/mol. The fiber diameters before and after calcination were on the order of 800 nm and 200 nm, respectively. A bead-on-string structure was obtained after electrospinning for M_W = 40,500 g/mol. As a result, the structure after calcination consisted of beads and beads with connected fibers. A variety of structures including solid fibers, micro-porous fibers and interconnected networks could be obtained after calcination. As the PVA/sol ratio was increased, thinner fibers were obtained up to about 20 vol% sol. At sol contents greater than 25 vol%, a fused structure was obtained. In general, uniformly distributed structures can be obtained by increasing the sol volume fraction or decreasing the polymer concentration. XRD analysis indicated hydroxyapatite to be the dominant inorganic phase remaining after calcination with an average crystal size between 10 to 30 nm. Electrospinning of the mixture reduces the crystal size in the order of 10 nm to 30 nm in the hydroxyapatite.